Neuronal Toll-like Receptor-4 regulation of Matrix Metalloproteinase-9 Activity Mediates Dentate Circuit Dysfunction after Traumatic Brain Injury

Deepak Subramanian[1#], Erick Contreras[1], Laura Dovek[2], Razieh Jaberi[1], Iryna M Ethell[2] and Vijayalakshmi Santhakumar[1#]

[1]Department of Molecular, Cell and Systems Biology, [2]Biomedical Sciences, University of California Riverside, Riverside, California 92521.

Keywords: Traumatic Brain Injury, Dentate gyrus, Toll-like Receptor 4, Matrix Metalloproteinase-9, Neuro-immune signaling, Synaptic plasticity

Abstract: 273 words Full Text Character count: 66,897 Number of pages: 47

Number of figures: 7 Supplementary figures: 4 Color figures: 10

Number of tables: 0 Number of supplementary tables: 3

Correspondence:
Deepak Subramanian, PhD
Department of Molecular, Cell and Systems Biology
University of California, Riverside
E-mail: dsubra@ucr.edu

Co-Correspondence:
Vijayalakshmi Santhakumar, PhD
Department of Molecular, Cell and Systems Biology
University of California, Riverside
E-mail: vijayas@ucr.edu

List of Abbreviations:

aCSF: Artificial Cerebrospinal Fluid

AMPAR: α-Amino-3-hydroxy-5-methyl-4-isoxazolepropionic Acid Receptor

ANOVA: Analysis of Variance

CA1 SR: CA1 Stratum Radiatum

CaMKIIa: Calcium/Calmodulin-Dependent Protein Kinase II Alpha

CreERT2: Cre Recombinase Estrogen Receptor T2

DG: Dentate Gyrus

DQ Gelatinase: Dye Quenched fluorogenic substrate for zymography

ECM: Extracellular Matrix

EPSC: Excitatory Postsynaptic Current

FPI: Fluid Percussion Injury

HMGB1: High-Mobility Group Box 1

IEI: Inter-Event Interval

IPSC: Inhibitory Postsynaptic Current

JSH-23: NF-κB Inhibitor

K-S test: Kolmogorov-Smirnov Test

LPS: Lipopolysaccharide

LTP: Long Term Potentiation

MMP-9: Matrix Metalloproteinase-9

NF-κB: Nuclear Factor Kappa B

TAK-242: TLR4 Antagonist

TBS: Theta Burst Stimulation

TBI: Traumatic Brain Injury

TTX: Tetrodotoxin

Abstract:

Neuroinflammatory pathways activated by traumatic brain injury (TBI) are critical mediators of long-term neurological dysfunction and represent promising therapeutic targets. Toll-like receptor 4 (TLR4), an innate immune receptor, was previously shown to contribute to seizure susceptibility and cognitive deficits in rats after lateral fluid percussion injury (FPI). However, the cellular and molecular mechanisms underlying TLR4-mediated circuit dysfunction early after brain injury is not fully understood. In this study, we define a cell- and circuit- specific neuroimmune-extracellular matrix signaling axis that mediates early post-TBI circuit dysfunction in the hippocampal Dentate Gyrus (DG). Using *ex vivo* electrophysiology in rat and mouse models one-week after brain injury, we demonstrate that neuronal TLR4 signaling regulates both excitatory and inhibitory synaptic inputs to dentate granule cells (DGC). Pharmacological inhibition of TLR4 in rats within 24 hours post-injury and cell-type-specific deletion of TLR4 in glutamatergic neurons in mice demonstrated that injury-driven excitatory circuit dysfunction is mediated by neuronal TLR4 and relies on downstream activation of Matrix Metalloproteinase-9 (MMP-9), an enzyme critical for extracellular matrix remodeling. In contrast, TLR4-dependent alterations in inhibitory inputs occurred independent of MMP-9, revealing a mechanistic divergence. Early inhibition of either TLR4 signaling or MMP-9 activity in rats within 24 hours post-injury reduced network hyperexcitability, improved long-term potentiation (LTP) in the dentate gyrus measured *in vivo* one-week after injury, and attenuated long-term deficits in spatial memory one-month post-injury. Furthermore, we demonstrate a context-dependent role for TLR4 signaling contributing to circuit homeostasis in the uninjured brain and driving

circuit dysfunction in the injured brain. Together, these results identify a novel TLR4 -MMP-9 axis as a key driver of early post-TBI dentate gyrus circuit dysfunction and behavioral deficits.

INTRODUCTION:

Traumatic brain injury (TBI) initiates a robust and complex inflammatory cascade that exacerbates secondary structural and functional damage [1–4]. While cellular damage is widespread and diffuse, the hippocampus is highly susceptible to post-traumatic pathology. Specifically, the hippocampal dentate gyrus (DG) undergoes extensive loss of hilar neurons and circuit reorganization that critically alters hippocampal network physiology and contributes to the development of cognitive impairments and post-traumatic epilepsy [5–11]. In this context, we previously identified a pivotal role for the neuronally expressed innate immune receptor, Toll-like receptor 4 (TLR4), in enhancing neuronal excitability and driving epileptogenesis after injury [12–14]. Yet, the downstream mechanisms by which specific immune receptors influence circuit physiology remain poorly understood.

Recent evidence indicates that canonical TLR4 activators, such as lipopolysaccharide (LPS) and high-mobility group box 1 (HMGB1), can upregulate Matrix Metalloproteinase-9 (MMP-9) activity in vitro [15,16]. MMP-9 , a zinc-dependent endopeptidase, is a critical regulator of synaptic communication and plasticity through the activity-dependent degradation of the extracellular matrix (ECM)[17–20]. Importantly, MMP-9 levels are elevated early in both animal models and clinical populations after brain injury [21–24] , driving pathological remodeling of synapses and circuits that promote epileptogenesis. [25–29]. Despite a strong temporal correlation between MMP-9 elevation and transient increases in TLR4 signaling after injury [12,30], a causal association between these two pathways has not been established. Based on the temporal correlation and shared

100 upstream activators, we hypothesized a mechanistic interaction between these two
101 pathways that contributes to the early circuit dysfunction after brain injury.

102 Here, we provide evidence for a novel mechanism involving TLR4-mediated upregulation of
103 MMP-9 activity following brain injury that drives maladaptive changes in synaptic
104 physiology, network excitability, and plasticity. Our findings reveal that the injury-induced
105 increase of MMP-9 in the dentate gyrus is specifically mediated by neuronal TLR4 signaling.
106 While TLR4-regulated MMP-9 activity was critical in enhancing excitatory synaptic inputs,
107 inhibitory input dysregulation was mediated by TLR4 signaling independent of MMP-9.
108 Furthermore, we demonstrate that this TLR4 and MMP-9 dependent pathway enhances
109 network excitability and impairs synaptic plasticity early after injury. Importantly, we show
110 that pharmacological inhibition of either TLR4 or MMP-9 effectively mitigates these early
111 pathological changes, highlighting the therapeutic potential of targeting this neuro-immune
112 signaling pathway to preserve circuit function after TBI.

113 **METHODS:**

114 All experiments were performed in accordance with IACUC protocols approved by the
115 University of California-Riverside, CA and in keeping with the ARRIVE guidelines. Male and
116 female Wistar rats (P23-P24) and mice (TLR4$^{f/f}$:CaMKIIa-CreERT2) were housed with
117 littermates in a 12-hour light/dark cycle with access to water and food ad libidum. All mice
118 were bred in-house. Animals were randomly assigned to either sham or FPI groups and
119 treatment conditions.

120 **Fluid Percussion Injury (FPI) and treatments**

121 Juvenile male and female Wistar rats (24 days old) were subjected to moderate (1.8-2.0 atm)
122 lateral FPI or sham injury using standard methods [12–14]. Briefly, a 2.7 mm hole was
123 trephined on the left side of the skull 3 mm caudal to bregma and 3.5 mm lateral from the
124 sagittal suture. A Luer-Lok syringe hub with a 3 mm inner diameter was placed over the
125 exposed dura and bonded to the skull with cyanoacrylate adhesive. The animals were
126 returned to their home cage following recovery. One day later, animals were briefly
127 anesthetized with isoflurane and attached to a fluid percussion injury device (Virginia
128 Commonwealth University, Richmond, VA, Model 01-B) directly at the metal nozzle. A
129 pendulum was dropped to deliver a brief (20ms) 1.9–2.0 atm impact on the dura. For sham
130 injury, the animals underwent surgical implantation of the hub and were anesthetized and
131 attached to the FPI device, but the pendulum was not dropped. Only rats with >10 seconds
132 apnea after injury were included in the injury group, and only the hemisphere ipsilateral to
133 the injury was examined.

134 To study the specific role of neuronal TLR4 signaling, $TLR4^{f/f}$:CaMKIIa-CreERT2 mice (8–10-
135 week-old male and female mice) were induced with tamoxifen and subjected to lateral FPI
136 (1.5 atm) or sham injury [31,32]. Tamoxifen (75mg/kg, i.p.) was prepared in 10% ethanol and
137 90% corn oil by sonicating at 37°C for 90 minutes. Mice received 3 doses of tamoxifen, 24
138 hours before injury, 30 minutes after injury and 24 hours after injury. TLR4 deletion in
139 glutamatergic neurons in dentate gyrus was confirmed through immunohistochemistry (see
140 immunohistochemistry methods below). Cre negative mice were used as genotype
141 controls. Animals were treated with vehicle (DMSO), TLR4 antagonist (TAK-242, 0.5mg/kg,
142 i.p., Invivogen, San Diego, CA) or MMP-9 antagonist (SB-3CT, 50mg/kg, i.p., SelleckChem,
143 Houston, TX) at 30 minutes, 8 hours, and 24 hours after injury.

144 **Ex vivo electrophysiology**

145 One-week after FPI or sham injury, animals were anesthetized with isoflurane and
146 decapitated. Coronal hippocampal slices (300 μm) were prepared in ice-cold sucrose
147 artificial cerebrospinal fluid (aCSF) containing (in mM): 85 NaCl, 75 sucrose, 24 NaHCO3,
148 25 glucose, 4 MgCl2, 2.5 KCl, 1.25 NaH2PO4, and 0.5 CaCl2 [33]. Slices were incubated at
149 32°C for 20 min in an interface holding chamber containing an equal volume of sucrose-
150 aCSF and recording aCSF containing (in mM) 126 NaCl, 2.5 KCl, 2 $CaCl_2$, 2 $MgCl_2$, 1.25
151 NaH_2PO_4, 26 $NaHCO_3$ and 10 D-glucose. All solutions were saturated with 95% O_2 and 5%
152 CO_2 and maintained at a pH of 7.4. Slices were allowed to equilibrate for an hour at room
153 temperature before recordings. Whole-cell voltage- and current-clamp recordings from
154 dentate granule cells (DGCs) were obtained at 33-34°C under IR-DIC (Olympus BX51 with
155 40x water immersion objectives) using 3-6MΩ glass pipettes fabricated using dual stage

156 glass micropipette puller (Narishige PC-10, Amityville NY). Data was recorded using
157 MultiClamp 700B amplifiers, digitized using Digidata 1440A and acquired using pClamp10
158 (Molecular Devices, San Jose, CA) at 10-kHz sampling frequency. Spontaneous and
159 miniature excitatory/inhibitory currents from the same DGCs were obtained using a cesium-
160 based internal solution (in mM: Cesium methanesulfonate 140, NaCl 5, HEPES 10, EGTA
161 0.2, Mg2ATP 2, Na2GTP 0.2, Qx314 5, (pH 7.25, 270-285 mOsm). Biocytin (0.2%) was
162 included in the internal solution for post hoc cell identification. Spontaneous and miniature
163 excitatory postsynaptic potentials (sEPSC and mEPSC) were recorded from the same
164 neurons at a holding potential of -70 mV, and spontaneous and miniature inhibitory
165 postsynaptic potentials (sIPSC and mIPSC respectively) were recorded at a holding
166 potential of 0 mV. Action potential independent miniature currents were isolated using
167 tetrodotoxin (TTX, 1μM). In a subset of experiments TLR4 signaling was selectively activated
168 by incubating slices in LPS-B5 ultrapure (Escherichia Coli serotype O55:B5, 10 μg/ml,
169 Invivogen, San Diego, CA), a selective TLR4 agonist, for 60-90 minutes before recording [34].
170 Data from cell in which access resistance changes over 20% during recordings and
171 recordings with access resistance above 25 MΩ were excluded from analysis.
172 Spontaneous/miniature synaptic currents (100 events/cell) were detected using template
173 search feature in Easy Electrophysiology (version 2.6., London, UK.) by a blinded investigator
174 and interevent intervals and amplitudes were analyzed as cumulative distribution in
175 Graphpad Prism 10.0.1 (Boston, MA).

176

177

178 **In vivo electrophysiology**

179 One-week after FPI/Sham injury rats were anesthetized under urethane (1.5g/kg i.p.) and
180 head-fixed onto a stereotaxic frame. Under aseptic conditions, rats were implanted with a
181 50 μm tungsten wire depth electrode (California Fine Wire company, Grover beach, CA) in
182 the granule cell layer (AP: 3-4 mm, ML: 2 mm, DV: 3-3.5 mm) guided by periodic electrical
183 stimulation of the angular bundle (ML:4-4.2 mm, DV: 1.8-2 mm; pulse width 150μs delivered
184 at 0.1Hz). Two screw electrodes on the contralateral side served as reference and ground.
185 The position of electrodes was secured using dental cement. Acute recordings from
186 urethane anesthetized rats started 60 minutes after induction. A current-response curve
187 was derived by electrical stimulation of the angular bundle (150 μs @ 0.1Hz). For assessing
188 Long Term Potentiation (LTP), DG LFP responses were evoked every 30 seconds for a period
189 of 30 minutes to derive baseline. LTP was induced by Theta Burst Protocol[35] and
190 responses were recorded for an additional 180 minutes. Signals were amplified 100 times
191 (Pinnacle systems, Lawrence, KS), sampled at 10kHz, digitized using PowerLab 16/35 and
192 recorded using LabChart8 software (AD Instruments, Colorado Springs, CO). Analysis was
193 conducted using LabChart modules. Dentate spikes were recorded from urethane
194 anesthetized rats (1.5g/kg i.p.) using 16 Ch silicon probe (A1x16-5mm-100-703 CM16,
195 Neuronexus, Ann Arbor, MI). Signals were amplified 100 times using Model 3600 amplifier
196 (AM-Systems, Sequim, WA), digitized using PowerLab 16/35 and recorded using Labchart8
197 Software (AD instruments, Colorado Springs, CO). Dentate spikes were detected using
198 Toothy analysis pipeline[36] (https://github.com/Farrell-Laboratory/Toothy). Briefly, large
199 positive events were identified using a 4.5 S.D. threshold. Detected events were visually

200 confirmed by a blinded investigator and the total number of dentate spikes recorded in a 30-
201 minute period were counted. We did not classify dentate spikes as type 1 or type 2.

202 **In Situ Zymography**

203 MMP-9 activity was evaluated in hippocampal slices obtained from rats and mice 48 hours
204 after injury using a modified in situ zymography protocol [37]. Briefly, sham/injured rats or
205 TLR4$^{f/f}$:CaMKIIa-CreERT2 mice and Cre^{-ve} controls were transcardially perfused using an
206 alcohol-based formalin free tissue fixative (Accustain, A5472 Sigma-Aldrich, St.Louis, MO),
207 embedded in 2% agar and coronal slices (50µm, VF-310-0Z Compresstome, Precisionary
208 Instruments, Ashland, MA) were prepared at <4°C to preserve enzyme activity. Slices were
209 then incubated with a fluorogenic Dye Quenched gelatin substrate (1:50 dilution, Invitrogen,
210 Waltham MA) for 40 min at 37°C, washed with PBS, fixed in 4% paraformaldehyde and
211 mounted on slides in Vectashield (Vector Labs, Newark, CA). The specificity of reactions
212 was confirmed by adding MMP-9 inhibitor SB-3CT to control slices (see supplementary
213 figure 2J-K). Semiquantitative analysis of DQ fluorescence in DG molecular layer were
214 performed using ImageJ by a blinded investigator. Data was collected from 2-4 slices /
215 animals and averaged. Intensity measures were normalized to CA1 stratum radiatum since
216 we did not observe any effect of injury, treatment or genotype in this region (Supplementary
217 figure 2B-C).

218 **Single molecule fluorescent in situ hybridization (RNAscope)**

219 To visualize TLR4 in mice and MMP-9 mRNA in rat, we used RNAscope Multiplex Fluorescent
220 in situ hybridization on cryosectioned slices (20µm). RNAscope Multiplex Fluorescent

221 Reagent kit v2 assay (ACD, Newark, CA) was used following the protocol for fixed tissue [38].
222 The following kits were used for this study: RNAscope Multiplex Fluorescent Reagent kit
223 (Cat#323100), RNAscope Probe-MM-TLR4 (Cat#316801) and RNAscope probe-Rn-MMP-9
224 (Cat#532281). Slices were coverslipped with DABCO with DAPI mounting media and imaged
225 using a Zeiss Axioscope and analyzed using QuPath software by a blinded investigator.

226

227 **Immunohistochemistry**

228 Male and female TLR4$^{f/f}$:CaMKIIa-CreERT2 mice (8-10 weeks) were induced with tamoxifen
229 as described above and subjected to Sham or FPI. Three days after injury, brain tissue was
230 harvested following transcardial perfusion with PBS followed by 4% PFA. Brains were post-
231 fixed overnight and then transferred to 30% sucrose until fully equilibrated. Tissue was
232 cryosectioned at 20 μm thickness and mounted on Superfrost Plus glass slides. For
233 immunohistochemistry, slides were brought to room temperature to remove OCT and
234 washed three times in PBS. Sections were permeabilized with 0.2% Triton X-100 in PBS for
235 45 minutes at room temperature, followed by blocking with 20% goat serum for 45 minutes.
236 Sections were then incubated overnight at 4 °C with a primary antibody against TLR4 (mouse
237 anti-TLR4; Santa Cruz Biotechnology; 1:250). After three PBS washes, sections were
238 incubated with goat anti-mouse Alexa Fluor 546 secondary antibody (1:1000, Thermo Fisher,
239 S11227) for 1 hour at room temperature. Slides were washed three times with PBS and
240 mounted using an antifade mounting medium. Images were acquired using a Zeiss
241 Axioscope-5 with stereo investigator (MBF Bioscience) from three animals per group, with

242 six sections analyzed per animal. Quantification was performed using ImageJ software by
243 calculating the Corrected Total Cell Fluorescence (CTCF) in the granule cell layer and hilus
244 for each section (Supplementary figure 2C-E).

245 **Behavioral Experiments**

246 Rats were trained on Barnes Maze task to assess spatial learning 1-month post-injury. The
247 Barnes maze table (Maze Engineers, https://conductscience.com/maze/) was 122 cm in
248 diameter with 20 holes (10 cm each). The target hole was equipped with an escape box (22.5
249 cm x 14 cm x 9 cm LxWxH). The maze table was set up within black curtain walls with visual
250 cues and a camera installed above to record animal movement. Two bright floodlights and
251 a fan served as aversive stimuli to encourage animals reach the escape box. Animals were
252 held in their home cage outside the curtain in a dark room until their turn to run the trial. On
253 day 1, rats were habituated to the behavior room for at least 1 hour and then placed in the
254 middle of the table inside starter cup for 1 minute following which they were allowed to
255 explore the table for 180 seconds. At the end of the trial, animals were gently guided to their
256 designated escape hole. The escape hole locations were randomly assigned to each rat and
257 remained the same till the end of the experiment. The table was thoroughly wiped with
258 ethanol between tests to eliminate odor cues. Rats were subjected to a single 180-second
259 trial for 3 days. Task acquisition and retention were confirmed through tests on day 4 and
260 day 7. Four rats that fell from the table and exhibited signs of lethargy were removed from
261 the test and sacrificed. Behavioral analysis was performed by a blinded experimenter using
262 Any-maze software. Parameters such as latency to escape hole, distance travelled and
263 spatial search strategy were evaluated between sham and injured rats. Spatial search

264 strategies were scored based on 11-point scoring scheme[39]. Thigmotaxis was quantified
265 by defining a peripheral zone of the testing arena that was approximately 12 cm from the
266 apparatus's outer edges. The proportion of time the animals spent within this designated
267 zone was recorded and used as the metric for thigmotaxis.

268

269

270 **Statistics**

271 Data are presented as mean ± standard error of the mean (SEM) for parametric measures,
272 or as median and interquartile range (IQR) where non-parametric distributions were
273 observed. To ensure rigorous data interpretation and minimize investigator bias, all data
274 analysis, including quantification of in situ zymography, electrophysiological recordings,
275 and behavioral scoring, was performed by researchers blinded to the treatment groups and
276 genotypes.

277 Normality of data distributions was assessed using the Shapiro-Wilk test. For the analysis
278 of synaptic events (sEPSC, mEPSC, sIPSC, and mIPSC), cumulative probability distributions
279 of inter-event intervals (IEI) and amplitudes were compared across groups using equal
280 number of consecutive events with the non-parametric Kolmogorov-Smirnov (K-S) test.
281 Effect sizes for these distributions were calculated using Cohen's d. Differences between
282 two groups were evaluated using two-tailed unpaired t-tests. For experiments involving
283 multiple factors, such as injury and drug treatment or injury and genotype, two-way ANOVA
284 or two-way repeated measures (RM) ANOVA (for input/output curves and behavioral training

285 days) were employed, followed by Šídák's multiple comparisons test where appropriate.

286 Significance was defined at $P<0.05$. Statistical analyses were performed using Graphpad

287 Prism 10.0.1 (Boston, MA).

288

289

290 **RESULTS:**

291 **Neuronal TLR4 signaling is necessary for early excitatory circuit changes after brain**
292 **injury.**

293 Prior studies have identified TLR4 contribution to early changes in glutamatergic synapse
294 strength after brain injury [12–14]. However, the nature of early circuit reorganization after
295 brain injury in the dorsal hippocampus and whether immune signaling regulates these
296 changes has not been examined. Whole-cell voltage clamp recordings from DGCs in dorsal
297 hippocampal slices one-week after FPI revealed an early decrease in the inter-event
298 intervals (IEI) of spontaneous excitatory postsynaptic currents (sEPSCs), indicating an
299 increase in sEPSC frequency (IEI in milliseconds: $Sham_{DMSO}$ mean – 336.9±13.93, median-
300 216.4, IQR- 86.05-429.9; FPI_{DMSO} mean – 225.3±8.26, median-144.8, IQR- 64.60-307.4., *n* =
301 8 cells/ group, *P*<0.0001 by K-S test, Cohen's *d* = 0.34, Figure 1A-E). Additionally, we
302 observed a reduction in sEPSC amplitude in DGCs from rats after brain injury (Amplitude in
303 pA: $Sham_{DMSO}$ mean – 13.16±0.17, median-12.20, IQR- 9.98-15.36; FPI_{DMSO} mean –
304 11.23±0.16, median-10.31, IQR- 8.05-13.42, *n* = 8 cells/ group, *P*<0.0001 by K-S test,
305 Cohen's *d* = 0.41). To assess potential post-traumatic synaptic reorganization, we recorded
306 action potential-independent miniature EPSCs (mEPSCs) in DGCs the presence of
307 tetrodotoxin (TTX, 1 μM). Similar to sEPSCs, DGCs in rats one week after FPI exhibited
308 shorter mEPSC IEI and smaller mEPSC amplitudes compared to Sham controls (IEI in
309 milliseconds: $Sham_{DMSO}$ mean: 824.8±34.17, median: 496.1, IQR:208.1-1096; FPI_{DMSO} mean:
310 642.4±28.91, median: 396.4, IQR: 158.2- 858.6; Amplitude in pA: $Sham_{DMSO}$ mean:
311 14.16±0.25, median:12.32, IQR: 8.90-17.91; FPI_{DMSO} mean: 9.28±0.16, median: 8.02, IQR:

312 6.55-10.55, *n* = 7 cells/ group, *P* <0.001 by K-S test, Cohen's *d* = 0.22 for IEI and 0.85 for
313 amplitude, Supplementary figure 1A-C). Together, these findings provide the first evidence
314 of an increase in excitatory synaptic inputs to DGCs in dorsal hippocampus of rats one
315 week after injury.

316 Significant changes in synaptic inhibition is often observed early after brain injury [5,7,40].
317 To evaluate whether inhibitory circuits are reorganized alongside the excitatory circuits, we
318 examined spontaneous inhibitory postsynaptic potentials (sIPSC) in the same neurons. In
319 contrast to changes in sEPSCs, sIPSC IEI was prolonged in DGCs from injured rats (IEI in
320 milliseconds: $Sham_{DMSO}$ mean: 190.3±6.64, median:128.1, IQR: 65.35- 252.4; FPI_{DMSO} mean:
321 256.6±9.272, median:181.1, IQR:83.78-320.4; n= 8 cells/group, *P* <0.0001 by K-S test,
322 Cohen's *d* = 0.29 Figure 1F-H). These findings indicate that in addition to receiving more
323 frequent excitatory inputs, the DGCs receive fewer inhibitory inputs after brain injury. DGCs
324 also showed an increase in sIPSC amplitude compared to sham controls after brain injury
325 (amplitude in pA: $Sham_{DMSO}$ mean: 16.66±0.35, median:13.78, IQR:10.81-19.21; FPI_{DMSO}
326 mean: 18.24±0.35, median: 15.74, IQR: 11.94-21.70, *n* = 8 cells/ group, *P* <0.0001 by K-S
327 test, Cohen's *d* = 0.16). These findings differ from our findings in the ventral hippocampus
328 demonstrating an increase in sIPSC frequency in DGCs after FPI [33,41,42]. We also
329 observed an increase in mIPSC amplitudes with no change in mIPSC IEI (Supplemental
330 Figure 1D-F). Together, these findings indicate an early dysregulation in excitatory and
331 inhibitory inputs to DGC's one-week after FPI. Furthermore, these results identify early
332 circuit reorganization after FPI and reveal potential differences in synaptic inhibition and
333 post-traumatic plasticity in the dorsal vs ventral hippocampus.

334 To determine whether inhibition of TLR4 signaling early after injury modified DGC synaptic
335 currents, we treated sham and FPI rats with TLR4 inhibitor TAK-242 (0.5mg/kg, i.p, 30 min, 8
336 hours and 24 hours post-injury). TAK-242 treatment reduced changes in sEPSC and mEPSC
337 frequency and amplitude in injured rats (Figure.1A-E, Supplementary figure 1A-C, and
338 Supplementary table.1). In addition, TAK-242 reduced injury-driven changes in sIPSC
339 frequency and mIPSC amplitude (Figure.1F-H, Supplementary figure 1D-F). These findings
340 demonstrate a role for TLR4 signaling in driving early synaptic dysregulation after FPI.

341 In contrast to injured animals, sham controls receiving TAK-242 showed paradoxically
342 opposing changes excitatory and inhibitory synaptic inputs to DGCs. In sham controls,
343 TAK-242 treatment reduced sEPSC IEI in DGCs, increasing frequency as observed after FPI
344 but failed to alter sEPSC amplitude (Figure 1B-E). Moreover, TAK-242 treated sham controls
345 showed a reduction in DGC sIPSC IEI and amplitude suggesting more frequent inhibitory
346 inputs (Figure 1F-H). Similar to sEPSCs, both mEPSC interval and amplitude were reduced
347 in TAK-242 treated sham controls (Supplementary figure 1A-C) consistent with synaptic
348 reorganization. However, Tak-242 treatment did not alter mIPSC frequency or amplitude.
349 Together, these findings identify a novel contribution of basal TLR4 signaling in maintaining
350 excitatory synaptic homeostasis in uninjured animals.

351 Our previous studies demonstrated neuronal TLR4 signaling as critical for post-traumatic
352 increase in DGCs AMPA currents [13]. To test whether the glutamatergic circuit changes
353 identified above require neuronal TLR4 signaling, we examined changes in sEPSC
354 frequency and amplitude in mice with selective deletion of TLR4 in CaMKII expressing
355 excitatory neurons (TLR4$^{fl/fl}$-CaMKIIa-CreERT2 mice). Care was taken to avoid constitutive

356 and developmental effects by inducing Cre recombinase just prior to injury.
357 Immunostaining for TLR4 in mice three-days after FPI, following the 3-day tamoxifen
358 induction strategy, revealed strong immunostaining for TLR4 in the granule cell layer and
359 hilus of Cre^{-ve} mice which was absent in Cre^{+ve} mice, confirming TLR4 deletion in DGCs (n =
360 3 mice/ group, $P<0.05$ by Nested t test, Supplementary figure 2A-C). Examination of active
361 and passive properties of DGCs revealed a significant decrease in capacitance and an
362 increase in firing frequency in Cre^{+ve} sham mice compared to Cre^{-ve} sham mice (n = 7 cells/
363 group, $P<0.05$ by two-way ANOVA, Supplementary figure 2E&I). We did not observe any
364 genotype effects on the resting membrane potential, input resistance or rheobase of DGCs
365 in sham controls (Supplementary figure 2F-H). Consistent with our previous reports in rat
366 and mice [31,43], there were no injury effects on DGC active properties in either genotype.
367 However, while there was no injury effect on DGC resting membrane potential in Cre^{-ve}
368 mice, DGCs from Cre^{+ve} mice with TLR4 deletion were more depolarized (Supplementary
369 figure 2F). Similar to our findings in rat, brain injury reduced DGC sEPSC IEI and amplitude
370 in Cre^{-ve} mice with intact TLR4 signaling (See Supplementary table 1; n = 7 cells/ group,
371 $P<0.0001$ by K-S test, Figure 1I-L). Additionally, DGC sEPSC IEI and amplitude were not
372 different between Cre^{-ve} and Cre^{+ve} sham injured mice. Importantly, although DGCs from
373 Cre^{+ve} mice with conditional deletion of TLR4 in excitatory neurons showed a small
374 decrease in sEPSC amplitude, they failed to exhibit injury-induced decrease in sEPSC IEI.
375 These findings demonstrate that TLR4 expression in glutamatergic neurons is necessary for
376 the early injury-driven changes in excitatory synaptic inputs to DGCs.

377

378 **MMP-9 activity is required for TLR4-dependent changes in DGC excitatory synapses**
379 **after brain injury**

380 We next sought to identify downstream molecular mechanisms through which TLR4
381 signaling dysregulates DGC synaptic inputs after brain injury. Several studies have reported
382 an upregulation in Matrix Metallproteinase-9 (MMP-9) expression in pre-clinical models of
383 TBI [27,30,44]. MMP-9 is a critical regulator of synaptic strength and plasticity [17,18], and
384 perturbations in MMP-9 activity is known to dysregulate synaptic physiology [19,37,45–48] .
385 Although extrinsic activation of TLR4 signaling has been shown to enhance MMP-9
386 expression in primary astrocyte/neuronal co-cultures and *in vivo* [15,16], whether TLR4
387 regulates MMP-9 activity and if this can induced synaptic and functional changes *in vivo*
388 and in the injured brain remains to be determined. Moreover, whether *neuronal* TLR4
389 regulates MMP-9 activity has not been examined.

390 To directly assess MMP-9 activity, we performed *in-situ* zymography on hippocampal slices
391 obtained from sham/FPI rats 48 hours after injury, focusing on the DG molecular layer
392 where the afferent glutamatergic synapses are located. DQ-fluorescence intensity values
393 were normalized to CA1 Stratum Radiatum (SR) since no changes were observed in this
394 region with injury, treatment or genotypes (Supplementary figure 2L-M, see methods). Our
395 experiments identified a significant increase in the MMP-9 activity in the DG molecular
396 layer in brain-injured rats compared to sham controls (MMP-activity normalized to CA1 SR:
397 Sham:14.56±2.15%, FPI:30.43±2.89%, n = 5 sham and 6 FPI rats, Figure 2A-C).
398 Pharmacologically blocking TLR4 early after FPI reduced MMP-9 activity in the DG of brain
399 injured rats ($Sham_{TAK-242}$: 17.22±2.68%, $FPI_{TAK-242}$: 16.36±2.97%, n = 5 Sham and 6 FPI rats;

400 Effect of Injury x Treatment F (1,18) = 9.13; P <0.05 by Two-way ANOVA). In contrast, MMP-9
401 activity in sham controls treated with TAK-242 was not different from vehicle treated sham
402 controls. These results identify TLR4 regulation of MMP-9 activity in the injured brain.

403 To isolate the role of neuronal TLR4 in regulating MMP-9 activity, we performed in-situ
404 zymography on mice with neuronal TLR4 deletion (TLR4$^{fl/fl}$-CaMKIIa-CreERT2) and Cre^{-ve}
405 controls (Supplementary figure 2A-C) 48 hours after Sham or FPI. We did not observe any
406 difference in MMP-9 activity between Cre^{-ve} sham and Cre^{+ve} sham mice, indicating that
407 TLR4 deletion does not alter normal MMP-9 levels without injury (Figure 2D-F). While Cre^{-ve}
408 mice showed an increase in MMP-9 levels after injury, mice with selective TLR4 deletion in
409 glutamatergic neurons failed to develop elevated MMP-9 activity after FPI (MMP-activity
410 normalized to CA1 SR: Cre^{-ve} Sham: 13.43±3.36%, Cre^{-ve} FPI: 42.79±5.02%; Cre^{+ve} SHAM:
411 10.59±3.15%, Cre^{+ve} FPI: 12.20±1.16%., n=3-4 mice/group; Effect of Injury x Genotype, F
412 (1,11) = 14.70; P<0.05 by Two-way ANOVA, Figure 2D-F). These findings demonstrate that
413 neuronal TLR4 is necessary for the post-injury upregulation of MMP-9 activity.

414 Next, we tested the possibility that TLR4 signaling increased MMP-9 levels through
415 transcriptional upregulation. Naïve rats (P30) were injected with a selective TLR4 agonist,
416 LPS-B5 (5mg/kg., i.p.) or saline and euthanized after six hours for single molecule
417 fluorescent in situ hybridization (smFISH) to quantify MMP-9 mRNA levels. Sections from
418 LPS-B5 injected rats showed a significant increase in MMP-9 mRNA in DGCs, indicating
419 that TLR4 activation enhances MMP-9 via transcriptional upregulation (intensity A.U/μm^2:
420 saline controls 1.67±0.15; LPS-B5 treated 2.41±0.19; n= 5/group, Figure 2H-J).
421 Furthermore, inhibition of NF-κB, a key downstream effector of TLR4, using JSH-23 (10

422 mg/kg) administered one hour before LPS-B5 injection abolished the upregulation of MMP-
423 9 (intensity A.U/μm^2 : JSH-23 + LPS-B5 1.319±0.16, n = 5 rats, Main effect F(2,12) =11.20, *P*
424 = 0.002, Figure 2G-I) Together, these findings identify TLR4 and NF-κB dependent
425 transcriptional upregulation of MMP-9 as a candidate mechanism for increase in MMP9
426 activity in the DG following brain injury.

427 Extracellular matrix (ECM) remodeling by MMP-9 has been shown to play a crucial role in
428 plasticity of excitatory and inhibitory synapses [49]. Therefore, we reasoned that TLR4
429 mediated increase in MMP-9 activity may be required for the post-traumatic changes in
430 synaptic inputs to DGCs. To examine the acute effects of TLR4 signaling *ex vivo*, we
431 compared sEPSCs in hippocampal slices from sham rats incubated in LPS-B5 (10 μg/ml for
432 90min) or aCSF. Acute LPS-B5 incubation significantly reduced sEPSC IEI and increased
433 sEPSC amplitude in DGCs mimicking the FPI phenotype (IEI in milliseconds: LPS-B5
434 incubation mean: 265.3±10.99, median:157.3, IQR: 69.18-330.4; Amplitude in pA: mean –
435 17.86±0.21, median-17.29, IQR- 14.06-21.09; *n* = 8 cells from 4 rats, Sham vs LPS-B5
436 incubated *P* <0.0001 by K-S test, Figure 3A-D). Unlike sEPSCs, acute TLR4 activation failed
437 to alter sIPSC frequency or amplitude in DGCs (Supplementary figure 3A-C). Importantly,
438 inhibiting MMP-9 using SB-3CT (10 μM) mitigated LPS-B5-induced changes in sEPSC IEI
439 and amplitude, indicating that TLR4-mediated alterations in excitatory synaptic inputs to
440 DGCs require MMP-9 activity (IEI in milliseconds:SB-3CT+LPS-B5: mean: 339.7±12.40,
441 median:230.9, IQR: 94.53-434.6; amplitude in pA: mean: 15.90±0.19, median:14.66, IQR:
442 11.53-18.96; *n* = 9 cells from 4 rats, LPS-B5 incubated vs SB-3CT+LPS-B5 *P* <0.0001 by K-S
443 test, Figure 3A-D).

444 Since we find that TLR4-mediated alterations in DGC sEPSC frequency requires MMP-9
445 activity, we tested if systemic inhibition of MMP-9 using SB-3CT treatment (50 mg/kg, i.p.)
446 early after FPI would prevent post-traumatic changes in excitatory inputs to DGCs. SB-3CT
447 treatment effectively mitigated injury-induced the changes in sEPSC IEI and amplitude
448 one-week after FPI in rat (see Supplementary table.1, Figure 3E-H). Consistent with our
449 findings in rat, SB-3CT treatment reduced post-injury changes in sEPSC IEI in DGCs from
450 Cre^{-ve} -negative $TLR4^{fl/fl}$-CaMKIIa-CreERT2 mice (Figure 3I-L). Note that Cre^{+ve} $TLR4^{fl/fl}$-
451 CaMKIIa-CreERT2 mice did not show difference in sEPSC intervals or amplitudes after FPI.
452 SB-3CT treatment did not have any effect on sIPSC frequency or amplitude (Supplementary
453 figure 3G-I) after FPI but enhanced sIPSC amplitude in sham controls suggesting that TLR4
454 regulation of DGC inhibitory synaptic parameters after injury does not require MMP-9
455 activation. Together, these results indicate that injury-driven changes in excitatory inputs to
456 DGCs required both TLR4 signaling and MMP-9 activity.

457 **Early activation of TLR4 - MMP-9 molecular axis contributes to DG network**
458 **dysfunction after brain injury**

459 Having established that the TLR4- MMP-9 mechanistic axis increases glutamatergic inputs
460 to DGCs after brain injury, we examined the contribution of this molecular pathway to early
461 changes in DG circuit function in rats *in vivo* one-week after brain injury. Input/output plots
462 of the DG population spike amplitude elicited in response to perforant path stimulation at
463 increasing current intensities, recorded under urethane anesthesia and normalized to peak
464 amplitude, revealed a leftward shift after FPI indicating increased network excitability (n = 6
465 SHAM and 5 FPI rats; Effect of injury – $F(1,9) = 6.462$, $P = 0.031$ by Two-way RM ANOVA,

466 Figure 4A-C). This increase in network excitability was mitigated by early inhibition of either
467 TLR4 signaling or MMP-9 activity, demonstrating their contribution in promoting post-
468 traumatic DG circuit dysfunction (n= 5-6 rats/group; Effect of Stimulus x Treatment: F
469 (6,166,40.08) = 4.752, *P*=0.0009 by Two-way RM ANOVA, Figure 4D). Paradoxically, as
470 previously reported in slices [12–14], TAK-242 treatment increased DG population spike
471 amplitude in sham controls (Figure 4E). However, consistent with its lack of effect on EPSC
472 frequency in sham controls, SB-3CT treatment did not alter DG network excitability in sham
473 rats (Figure 4E).

474 Enhanced network excitability combined with deficits in synaptic inhibition can increase
475 dentate throughput. We assessed DG throughput by examining dentate spikes, a distinct
476 DG population event driven by entorhinal cortex[50,51] . Linear 16- channel silicon probe
477 recordings of dentate spikes in anesthetized rats (Figure 4F-G) revealed a significant
478 increase in the frequency of dentate spikes one-week after FPI (in Hz: Sham: 0.11±0.019;
479 FPI 0.24±0.025, n = 4-5 rats/group, *P*= 0.006 by two tailed unpaired t-test), identifying
480 enhanced dentate throughput following FPI. To test if inhibition of either TLR4 signaling or
481 MMP-9 activity early after injury would reduce changes to DG throughput, we examined
482 dentate spikes in TAK-242 or SB-3CT treated sham/injured rats. Our experiments
483 demonstrate that early inhibition of either TLR4 signaling or MMP-9 activity effectively
484 prevented the post injury increase in dentate spike frequency without impacting it in sham
485 controls (n = 4-5 rats/group; Effect of Interaction F (2,21) = 9.975, *P*<0.001 by Two-way
486 ANOVA, Figure 4G).

487 We previously demonstrated that early post-injury increase in DGC calcium permeable
488 AMPA currents and deficits in working memory were mitigated by TLR4 inhibition [13]. To
489 assess whether the TLR4-MMP9 signaling impacts synaptic plasticity, long-term
490 potentiation (LTP) at perforant path-DGC synapses in anesthetized rats *in vivo* using theta-
491 burst stimulation (TBS) [35]. In the first 10 minutes after TBS, the field EPSP slope
492 normalized to the maximum slope at baseline trended lower but was not statistically
493 different between sham and FPI. However, there was a reduction in the field EPSP slope at
494 60 min, 120 min, and 180 min post-TBS indicating impairment in LTP maintenance (n = 6
495 rats/group, Two-way RM ANOVA with Šídák's multiple comparisons 10 min: P =0.065, 60
496 min: P = 0.003, 120 min: P = 0.002, 180 min: P = 0.125, Figure 5A-G). Crucially, early in vivo
497 antagonism of either TLR4 or MMP-9 early after FPI effectively prevented deficits in LTP in
498 injured rats, demonstrating contribution of TLR4-MMP-9 axis to LTP deficits after brain
499 injury (See Supplementary table 2, Figure 5A-G). Consistent with the paradoxical effects of
500 TAK-242 on sEPSC and network excitability in sham controls, TAK-242 treatment resulted in
501 deficits in LTP in sham rats (Figure 5F-G). Once again, unlike TAK242, SB-3CT treatment
502 failed to impact LTP Sham rats, paralleling on the differential effects of the treatments on
503 sEPSC frequency, population spike amplitude and dentate spike frequency in sham
504 animals. These findings demonstrate that TLR4-MMP-9 dependent post-traumatic circuit
505 changes compromise DG glutamatergic circuit function and plasticity.

506 **Targeting TLR4 or MMP-9 axis early after brain injury limits long-term spatial memory**
507 **impairments.**

508 Since we identify post injury increase in dentate spikes which can compromise hippocampal
509 information processing [52–55], and blocking TLR4 and MMP-9 early after injury prevent this
510 change, we sought to determine if TLR4 and MMP-9 antagonists could alleviate long term
511 cognitive deficits after brain injury. We adopted a Barnes maze spatial learning task which
512 has been shown to rely on intact DG function[56,57]. One month after sham/FPI, brain
513 injured rats exhibited a longer latency to find the escape hole and traveled a greater total
514 distance compared to sham controls, early during training but reached control levels of task
515 performance by Day 3 (See Supplementary table 3, *n* =10 rats / group, $P<0.05$ by TW-RM
516 ANOVA, Figure 6A-E). Additionally, there was no difference in task performance during trials
517 on Day 4 and Day 7, indicating that task retention is not impaired (Supplementary figure 4A-
518 D). Although there were no differences in speed of locomotion (Supplementary figure 4E),
519 injured rats showed increased thigmotaxis on Days 1 and 2 (Time spent in thigmotaxis zone
520 in seconds: $Sham_{DMSO}$ – 24.73±5.42, FPI_{DMSO} – 64.99±16.96; *n*= 10 rats/group, Effect of injury–
521 F (1,18) = 6.841, $P<0.05$ by Two-way -RM ANOVA, Figure 6, E, I). Since injured rats showed a
522 significant increase in both thigmotaxis and latency to find the escape on Day 2 of task
523 acquisition, we examined the use of spatial strategy for navigation using a 11-point scoring
524 system [39]. Analysis of search strategies on Day 2 showed that injured animals employed
525 random or serial strategies more often, demonstrating specific deficits in ability to recall
526 spatial cues for navigation (Search strategy score_Day2: $Sham_{DMSO}$ – 7.7±0.73, FPI_{DMSO} –
527 2.4±0.47; *n*= 10 rats/group, Effect of injury– F (1,18) = 17, $P<0.01$ by Two-way RM ANOVA,
528 Figure.6A-C). These results suggest a mild delay in task acquisition after brain injury which
529 is apparent on Day 2 of the task.

530 We focused our analysis on Day 2 of task acquisition when the injury-induced impairment is
531 most apparent. Early inhibition of TLR4 signaling or MMP-9 activity prevented post-injury
532 changes in latency to escape, and distance traveled observed on Day 2 (n = 6-10 rats/group;
533 $P<0.05$ by Two-way RM ANOVA, Supplementary table 3 and Figure 6F-G). Furthermore, the
534 search strategy scores significantly improved with MMP-9 inhibition. While TLR4 inhibition
535 trended to improve the strategy score, the difference did not reach statistical significance
536 (Figure 6H). Importantly, while MMP-9 did not have any adverse effects on sham controls,
537 TLR4 inhibition showed a trend towards increased latency, distance travelled and
538 thigmotaxis, and a lower spatial search strategy score (Figure 6F-I) which did not reach
539 statistical significance. Collectively, these findings demonstrate that early inhibition of the
540 TLR4-MMP-9 signaling axis effectively mitigates mild long term spatial learning deficits
541 observed after FPI.

542

543

544 **DISCUSSION**:

545 Understanding how inflammatory pathways modulate neuronal function after brain injury
546 is critical for developing effective therapeutic strategies to minimize the long-term
547 sequelae of TBI. While widespread secondary injury is driven by glial mediators of
548 neuroinflammation [1,2], we previously showed that the neuronal expression of innate
549 immune receptor TLR4 is upregulated in the hippocampus early after injury, contributing to
550 long-term seizure susceptibility and impaired working memory [12–14]. Here, we provide

551 mechanistic evidence that TLR4 signaling mediates rapid, circuit-level changes in both
552 excitatory and inhibitory synaptic transmission after injury. Using a combination of
553 pharmacology in rats and mouse genetics we demonstrate a central role for TLR4
554 expressed in CaMKII-positive excitatory neurons in mediating the observed circuit changes
555 through the upregulation of MMP-9. Importantly, we show that TLR4 or MMP-9 inhibition
556 early after brain injury not only reduces these pathological changes one-week after injury,
557 but improves deficits in spatial learning 1-month after injury.

558 **TLR4 Signaling Augments Glutamatergic inputs to DGCs after brain injury.**

559 TLR4 signaling is well established as a driver of neuronal excitability [3,58–62]. Our prior
560 work showed that TLR4 signaling enhances AMPA currents in granule cells contributing to
561 DG network hyperexcitability [12,13]. Examining circuit-level changes in injured animals
562 one week after injury, this study identifies an aberrant increase in excitatory inputs to DGCs
563 in the dorsal hippocampus. Considering that perforant path fibers are severed in coronal
564 hippocampal slice preparations [63], the post-injury increase in spontaneous EPSCs and
565 action potential-independent miniature events observed here indicate an increase in
566 synaptic contacts, consistent with early axonal sprouting [42], or elevated mossy cell
567 excitability previously reported after FPI [64]. Our findings highlight a critical role of TLR4
568 signaling in this process. First, we show that early pharmacological inhibition of TLR4
569 mitigates changes in both spontaneous and miniature EPSCs. We further demonstrate that
570 transient activation of TLR4 signaling in acute brain slices using LPS-B5 is sufficient to
571 augment sEPSCs frequency to levels comparable to those seen in injured animals.
572 Furthermore, by leveraging TLR4$^{fl/fl}$: CaMKIIa-CreERT2 mice, we demonstrate that selective

573 deletion of TLR4 in glutamatergic neurons alone is sufficient to mitigate the post-injury
574 increase in sEPSC frequency. Together, these findings show that neuronal TLR4 is both
575 necessary and sufficient to enhance glutamatergic drive to DGCs after brain injury.

576 **A Novel Neuro-Immune-Extracellular Matrix Signaling Cascade Underlies Early Post-**
577 **Traumatic Glutamatergic Circuit Plasticity**

578 To mechanistically elucidate how TLR4 enhances glutamatergic drive to DGCs after injury,
579 we focused on MMP-9 as a potential downstream effector. MMP-9 co-localizes with
580 excitatory synapses in an activity-dependent manner, and increased MMP-9 activity is
581 known to dysregulate glutamatergic synaptic transmission [37,49,65–67]. We previously
582 reported that neuronal TLR4 enhances calcium-permeable AMPA currents in DGCs post-
583 injury by increasing the surface expression of GluA1 subunits [13]. Notably, MMP-9 activity
584 has been shown to regulate AMPA receptor mobility and synaptic accumulation of GluA1
585 subunits following chemically induced LTP [68]. In addition, TLR4 ligands such as high-
586 mobility group box 1 (HMGB1) and lipopolysaccharide (LPS) are known to enhance MMP-9
587 expression in cultures and following ischemic insult [15,16].

588 Here, we show that pharmacologically inhibiting TLR4 signaling (rats) or deleting TLR4 in
589 excitatory neurons (mice) both limit post-injury increases in MMP-9 activity. By using LPS-
590 B5 to selectively activate TLR4, we demonstrate that activation of TLR4 alone increases
591 MMP-9 mRNA levels in the dentate gyrus of naïve rats in an NF-κB dependent manner.
592 Thus, as summarized in Figure 7, our findings identify a novel TLR4/NF-κB-dependent
593 transcriptional pathway that upregulates MMP-9 activity and promotes glutamatergic

594 circuit reorganization following brain injury. Consistent with this, inhibition of MMP-9 with
595 SB-3CT effectively reduced the glutamatergic changes driven by both direct activation of
596 TLR4 signaling in slices (LPS-B5) and in vivo following brain injury.

597 **Mechanistic Divergence in TLR4 regulation of glutamatergic and GABAergic circuits**

598 In contrast to the glutamatergic inputs, we observed a decrease in the frequency of
599 inhibitory inputs to DGCs one week after FPI. This stands in direct contrast to our previous
600 findings from the ventral hippocampus [33,41,42], highlighting potential regional
601 differences in functional plasticity between dorsal and ventral hippocampal inhibitory
602 circuits [69]. While TLR4 inhibition reduced post-traumatic changes in IPSCs, this effect
603 was independent of MMP-9 activity. Excessive MMP-9 activity was previously implicated in
604 PV hypofunction and perineuronal net remodeling underlying auditory hypersensitivity in
605 the mouse model of Fragile X Syndrome, a neurodevelopmental disorder associated with
606 autism [70]. However, our findings indicate a divergence of TLR4-dependent mechanisms
607 of circuit reorganization, with MMP-9-independent mechanisms contributing to changes in
608 inhibitory synapses (Figure 7). Furthermore, selective activation of TLR4 with LPS-B5 did
609 not alter sIPSC frequency in DGCs. Therefore, it is possible that injury-driven loss of hilar
610 interneurons contributes to the reduction in sIPSC after brain injury [7,43]. However, we
611 observed an increase in mIPSC frequency following LPS-B5 suggesting perturbations in
612 release probability or presynaptic calcium [40,71–73]. Future studies should determine
613 whether neuronal or glial TLR4 is involved in post-injury changes in inhibition and its
614 functional impact on dentate function and behaviors.

615 **Network Consequences and behavioral impact of TLR4/MMP-9 pathway.**

616 The dentate gyrus plays a central node in hippocampal memory processing, regulating the
617 flow of information through the hippocampal circuitry [53,74,75]. Thus, perturbations in DG
618 circuit function can directly impair cognitive processes. Our earlier studies showed
619 enhanced perforant path evoked EPSC amplitude suggesting stronger entorhinal-dentate
620 coupling in the injured brain and deficits in working memory [12–14]. Here we advance
621 these findings using in vivo approaches to identify increased dentate network excitability
622 early after injury. Furthermore, although the LTP induction was unaffected, LTP
623 maintenance was compromised in injured rats suggesting that the strengthening of
624 perforant path to granule cell synapses doesn't saturate synaptic strength and preclude
625 potentiation. Rather, we find selective deficits in LTP maintenance after brain injury
626 indicating altered transcriptional processes. Importantly, we report an increase in dentate
627 spike frequency early after brain injury indicating abnormal entorhinal-dentate throughput.
628 Since dentate spikes are critical in hippocampal information processing, memory
629 formation, and consolidation [50–54,76,77], abnormal dentate spikes could impair
630 memory processing after brain injury. Supporting this proposal, treatments that reduced
631 dentate spike frequency in injured animals also improved spatial learning deficits.
632 Crucially, dentate spikes are also increased in experimental models of epilepsy[78],
633 suggesting that these events may serve as biomarkers for post-traumatic epileptogenesis
634 alongside the pathological high frequency oscillations and altered sleep spindles identified
635 previously [79,80]. In summary, we find that inhibition of the novel TLR4-MMP9 signaling
636 axis after brain injury was effective in limiting post-traumatic deficits in dentate circuit

excitability, long term potentiation and spatial memory indicating therapeutic potential of manipulating this pathway (Figure 7).

A Novel Constitutive Role for TLR4 Signaling in Basal Circuit Homeostasis

Our study reveals a fundamental role for basal TLR4 signaling in maintaining dentate circuit homeostasis. We found that inhibition of TLR4 signaling in uninjured animals consistently altered synaptic inputs, network excitability, and plasticity. Specifically, timed and selective deletion of TLR4 in glutamatergic neurons in a mature circuit caused a genotype-dependent reduction in granule cell capacitance and increased firing rates (Figure 7). This indicates a constitutive role for neuronal TLR4 in limiting basal excitability. A reduction in capacitance with increased firing in the absence of changes in action potential threshold parallels observations in parvalbumin neurons in epilepsy models, where regulation of perineuronal nets alters neuronal firing through effects on cell capacitance[38,81,82]. Indeed, our prior studies have found that ability of TLR4 blockers to increase dentate excitability in uninjured controls is abolished when glial metabolic processes are disrupted[14]. Our finding that TLR4 or MMP9 antagonism does not impact dentate spike frequency in uninjured controls, is consistent with lack of TLR4 modulation of perforant path evoked AMPA currents in the absence of injury. Nevertheless, the basal TLR4 regulation of network homeostasis appears critical as blocking TLR4 enhances network excitability, impairs LTP maintenance and spatial memory (Figure 7). Future studies should examine the mechanisms underlying basal TLR4 regulation of neuronal activity.

657 Collectively, our data establishes the TLR4-NFκB-MMP-9 signaling axis as a central
658 mechanism driving post-TBI pathology. By placing MMP-9 as the downstream mediator for
659 TLR4-induced glutamatergic synaptic and network dysfunction, these findings provide a
660 novel and targetable therapeutic avenue for mitigating epileptogenesis and cognitive
661 deficits following traumatic brain injury.

662

663

Declarations

Ethics approval and consent to participate

All experiments were performed in accordance with IACUC protocols approved by the University of California-Riverside, CA (Approval number #20210005/35) and in keeping with the ARRIVE guidelines.

Consent for publication

Not applicable.

Availability of data and materials

All data are available from the corresponding author upon reasonable request.

Competing interests

The authors declare no competing interests.

Funding

This work is supported by National Institutes of Health (NIH) NINDS R01 NS069861, R01NS097750 to V.S., NIH/NINDS F31NS124290 to L.D; CDMRP- Epilepsy Research Program grant W81XWH-21-1-0684 to D.S.

Authors' contributions

D.S, E.C and L.D performed experiments; D.S, E.C, L.D, and R.J analyzed data; D.S, I.E and V.S interpreted results of experiments; D.S prepared figures; D.S, V.S conception and design of research; D.S and V.S drafted manuscript; D.S, I.E and V.S finalized and approved manuscript.

Acknowledgements: We thank Dr. Leszek Kaczmarek (Nencki Institute, Warsaw, Poland) for his expert advice on *in situ* zymography. We also thank Dr. Amanda Schott and Dr. Jordan S Farrell (Harvard Medical School) for their expertise and help with Dentate spike detection algorithms.

REFERENCES:

1. Sharma R, Leung WL, Zamani A, O'brien TJ, Espinosa PMC, Semple BD. Neuroinflammation in post-traumatic epilepsy: Pathophysiology and tractable therapeutic targets. Brain Sciences. 2019 Nov 1;9(11).

2. Mukherjee S, Arisi GM, Mims K, Hollingsworth G, O'Neil K, Shapiro LA. Neuroinflammatory mechanisms of post-traumatic epilepsy. Journal of Neuroinflammation. 2020 June 17;17(1).

3. Webster KM, Sun M, Crack P, O'Brien TJ, Shultz SR, Semple BD. Inflammation in epileptogenesis after traumatic brain injury. Journal of Neuroinflammation. 2017 Jan 13;14(1).

4. Simon DW, McGeachy MJ, Baylr H, Clark RSB, Loane DJ, Kochanek PM. The far-reaching scope of neuroinflammation after traumatic brain injury. Nature Reviews Neurology. 2017 Mar 1;13(3):171–91.

5. Lowenstein D, Thomas M, Smith D, McIntosh T. Selective vulnerability of dentate hilar neurons following traumatic brain injury: a potential mechanistic link between head trauma and disorders of the hippocampus. J Neurosci. 1992 Dec 1;12(12):4846–53.

6. McIntosh, Saatman, Raghupathi, Graham, Smith, Lee, et al. The Dorothy Russell Memorial Lecture* The molecular and cellular sequelae of experimental traumatic brain injury: pathogenetic mechanisms. Neuropathology Appl Neurobio. 1998 Aug;24(4):251–67.

7. Toth Z, Hollrigel GS, Gorcs T, Soltesz I. Instantaneous Perturbation of Dentate Interneuronal Networks by a Pressure Wave-Transient Delivered to the Neocortex. 1997.

8. Atkins CM. Decoding Hippocampal Signaling Deficits After Traumatic Brain Injury. Transl Stroke Res. 2011 Dec;2(4):546–55.

9. Hunt RF, Boychuk JA, Smith BN. Neural circuit mechanisms of post–traumatic epilepsy. Front Cell Neurosci [Internet]. 2013 [cited 2025 Nov 13];7. Available from: http://journal.frontiersin.org/article/10.3389/fncel.2013.00089/abstract

10. Paterno R, Folweiler KA, Cohen AS. Pathophysiology and Treatment of Memory Dysfunction After Traumatic Brain Injury. Curr Neurol Neurosci Rep. 2017 July;17(7):52.

11. Neuberger EJ, Gupta A, Subramanian D, Korgaonkar AA, Santhakumar V. Converging early responses to brain injury pave the road to epileptogenesis. Journal of Neuroscience Research. 2019 Nov 1;97(11):1335–44.

12. Li Y, Korgaonkar AA, Swietek B, Wang J, Elgammal FS, Elkabes S, et al. Toll-like receptor 4 enhancement of non-NMDA synaptic currents increases dentate excitability after brain injury. Neurobiology of Disease. 2015 Feb 1;74:240–53.

13. Korgaonkar AA, Li Y, Sekhar D, Subramanian D, Guevarra J, Swietek B, et al. Toll-like Receptor 4 Signaling in Neurons Enhances Calcium-Permeable α-Amino-3-Hydroxy-5-Methyl-4-Isoxazolepropionic Acid Receptor Currents and Drives Post-Traumatic Epileptogenesis. Annals of Neurology. 2020 Apr 1;87(4):497–515.

14. Korgaonkar AA, Nguyen S, Li Y, Sekhar D, Subramanian D, Guevarra J, et al. Distinct cellular mediators drive the Janus faces of toll-like receptor 4 regulation of network excitability which impacts working memory performance after brain injury. Brain, behavior, and immunity. 2020 Aug;88:381–95.

15. Yang CC, Lin CC, Hsiao LD, Kuo JM, Tseng HC, Yang CM. Lipopolysaccharide-induced matrix metalloproteinase-9 expression associated with cell migration in rat brain astrocytes. International Journal of Molecular Sciences. 2020 Jan 1;21(1).

16. Qiu J, Xu J, Zheng Y, Wei Y, Zhu X, Lo EH, et al. High-mobility group box 1 promotes metalloproteinase-9 upregulation through toll-like receptor 4 after cerebral ischemia. Stroke. 2010 Sept;41(9):2077–82.

17. Huntley GW. Synaptic circuit remodelling by matrix metalloproteinases in health and disease. Nature Reviews Neuroscience. 2012 Nov;13(11):743–57.

18. Ethell IM, Ethell DW. Matrix metalloproteinases in brain development and remodeling: synaptic functions and targets. Journal of neuroscience research. 2007 Oct;85(13):2813–23.

19. Szklarczyk A, Lapinska J, Rylski M, Mckay RDG, Kaczmarek L. Matrix Metalloproteinase-9 Undergoes Expression and Activation during Dendritic Remodeling in Adult Hippocampus. 2002.

20. Dityatev A, Schachner M. Extracellular matrix molecules and synaptic plasticity. Nature reviews Neuroscience. 2003 June;4(6):456–68.

21. Minta K, Brinkmalm G, Al Nimer F, Thelin EP, Piehl F, Tullberg M, et al. Dynamics of cerebrospinal fluid levels of matrix metalloproteinases in human traumatic brain injury. Sci Rep. 2020 Oct 22;10(1):18075.

22. Wang X, Jung J, Asahi M, Chwang W, Russo L, Moskowitz MA, et al. Effects of Matrix Metalloproteinase-9 Gene Knock-Out on Morphological and Motor Outcomes after Traumatic Brain Injury. 2000.

757 23. Hayashi T, Kaneko Y, Yu S, Bae E, Stahl CE, Kawase T, et al. Quantitative analyses of
758 matrix metalloproteinase activity after traumatic brain injury in adult rats. Brain
759 Research. 2009 July;1280:172–7.

760 24. Grossetete M, Phelps J, Arko L, Yonas H, Rosenberg GA. ELEVATION OF MATRIX
761 METALLOPROTEINASES 3 AND 9 IN CEREBROSPINAL FLUID AND BLOOD IN PATIENTS
762 WITH SEVERE TRAUMATIC BRAIN INJURY. Neurosurgery. 2009 Oct;65(4):702–8.

763 25. Reinhard SM, Razak K, Ethell IM. A delicate balance: Role of MMP-9 in brain
764 development and pathophysiology of neurodevelopmental disorders. Frontiers in
765 Cellular Neuroscience. 2015 July 29;9(JULY).

766 26. Vafadari B, Salamian A, Kaczmarek L. MMP-9 in translation: from molecule to brain
767 physiology, pathology, and therapy. Journal of Neurochemistry. 2016 Oct 1;139:91–
768 114.

769 27. Pijet B, Stefaniuk M, Kostrzewska-Ksiezyk A, Tsilibary PE, Tzinia A, Kaczmarek L.
770 Elevation of MMP-9 Levels Promotes Epileptogenesis After Traumatic Brain Injury.
771 Molecular Neurobiology. 2018 Dec 1;55(12):9294–306.

772 28. Wilczynski GM, Konopacki FA, Wilczek E, Lasiecka Z, Gorlewicz A, Michaluk P, et al.
773 Important role of matrix metalloproteinase 9 in epileptogenesis. Journal of Cell
774 Biology. 2008 Mar 10;180(5):1021–35.

775 29. Dityatev A, Fellin T. Extracellular matrix in plasticity and epileptogenesis. Neuron Glia
776 Biol. 2008 Aug;4(3):235–47.

777 30. Jia F, Pan Y hua, Mao Q, Liang Y min, Jiang J yao. Matrix metalloproteinase-9 expression
778 and protein levels after fluid percussion injury in rats: The effect of injury severity and
779 brain temperature. Journal of neurotrauma. 2010 June;27(6):1059–68.

780 31. Corrubia L, Huang A, Nguyen S, Shiflett MW, Jones MV, Ewell LA, et al. Early deficits in
781 dentate circuit and behavioral pattern separation after concussive brain injury.
782 Experimental Neurology. 2023 Dec;370:114578.

783 32. Witgen BM, Lifshitz J, Smith ML, Schwarzbach E, Liang SL, Grady MS, et al. Regional
784 hippocampal alteration associated with cognitive deficit following experimental brain
785 injury: A systems, network and cellular evaluation. Neuroscience. 2005;133(1):1–15.

786 33. Gupta A, Elgammal FS, Proddutur A, Shah S, Santhakumar V. Decrease in Tonic
787 Inhibition Contributes to Increase in Dentate Semilunar Granule Cell Excitability after
788 Brain Injury. J Neurosci. 2012 Feb 15;32(7):2523–37.

789 34. Hirschfeld M, Ma Y, Weis JH, Vogel SN, Weis JJ. Cutting edge: repurification of
790 lipopolysaccharide eliminates signaling through both human and murine toll-like
791 receptor 2. J Immunol. 2000 July 15;165(2):618–22.

35. Cooke SF, Wu J, Plattner F, Errington M, Rowan M, Peters M, et al. Autophosphorylation of αCaMKII is not a general requirement for NMDA receptor-dependent LTP in the adult mouse. Journal of Physiology. 2006 Aug;574(3):805–18.

36. Schott AL, Esfahany KN, Grocott JM, Farrell JS. Toothy: an interactive platform for dentate spike curation. bioRxiv. 2025 Oct 3;2025.10.03.680300.

37. Gawlak M, Górkiewicz T, Gorlewicz A, Konopacki FA, Kaczmarek L, Wilczynski GM. High resolution in situ zymography reveals matrix metalloproteinase activity at glutamatergic synapses. Neuroscience. 2009 Jan 12;158(1):167–76.

38. Proddutur A, Nguyen S, Yeh CW, Gupta A, Santhakumar V. Reclusive chandeliers: Functional isolation of dentate axo-axonic cells after experimental status epilepticus. Progress in Neurobiology. 2023 Dec;231:102542.

39. Rodríguez Peris L, Scheuber MI, Shan H, Braun M, Schwab ME. Barnes maze test for spatial memory: A new, sensitive scoring system for mouse search strategies. Behavioural Brain Research. 2024 Feb;458:114730.

40. Hunt RF, Scheff SW, Smith BN. Synaptic Reorganization of Inhibitory Hilar Interneuron Circuitry after Traumatic Brain Injury in Mice. J Neurosci. 2011 May 4;31(18):6880–90.

41. Gupta A, Dovek L, Proddutur A, Elgammal FS, Santhakumar V. Long-Term Effects of Moderate Concussive Brain Injury During Adolescence on Synaptic and Tonic GABA Currents in Dentate Granule Cells and Semilunar Granule Cells. Front Neurosci. 2022;16:800733.

42. Santhakumar V, Ratzliff ADH, Jeng J, Toth Z, Soltesz I. Long-term hyperexcitability in the hippocampus after experimental head trauma. Annals of Neurology. 2001 Dec;50(6):708–17.

43. Santhakumar V, Bender R, Frotscher M, Ross ST, Hollrigel GS, Toth Z, et al. Granule cell hyperexcitability in the early post-traumatic rat dentate gyrus: the 'irritable mossy cell' hypothesis. The Journal of Physiology. 2000 Apr;524(1):117–34.

44. Hadass O, Tomlinson BN, Gooyit M, Chen S, Purdy JJ, Walker JM, et al. Selective Inhibition of Matrix Metalloproteinase-9 Attenuates Secondary Damage Resulting from Severe Traumatic Brain Injury. PLoS ONE. 2013 Oct 23;8(10).

45. Michaluk P, Wawrzyniak M, Alot P, Szczot M, Wyrembek P, Mercik K, et al. Influence of matrix metalloproteinase MMP-9 on dendritic spine morphology. J Cell Sci. 2011 Oct 1;124(Pt 19):3369–80.

46. Wiera G, Szczot M, Wojtowicz T, Lebida K, Koza P, Mozrzymas JW. Impact of matrix metalloproteinase-9 overexpression on synaptic excitatory transmission and its

plasticity in rat CA3-CA1 hippocampal pathway. J Physiol Pharmacol. 2015 Apr;66(2):309–15.

47. Nagy V, Bozdagi O, Matynia A, Balcerzyk M, Okulski P, Dzwonek J, et al. Matrix metalloproteinase-9 is required for hippocampal late-phase long-term potentiation and memory. Journal of Neuroscience. 2006 Feb 15;26(7):1923–34.

48. Bozdagi O, Nagy V, Kwei KT, Huntley GW. In vivo roles for matrix metalloproteinase-9 in mature hippocampal synaptic physiology and plasticity. Journal of Neurophysiology. 2007 July;98(1):334–44.

49. Wiera G, Mozrzymas JW. Extracellular Metalloproteinases in the Plasticity of Excitatory and Inhibitory Synapses. Cells [Internet]. 2021 Aug 11;10(8). Available from: http://www.ncbi.nlm.nih.gov/pubmed/34440823

50. Bragin A, Jand& G, Nadasdy Z, Van Landeghem M, Buzsaki G. Dentate EEG Spikes and Associated Interneuronal Population Bursts in the Hippocampal Hilar Region of the Rat. Vol. 73, JOURNALOF NEUROPHYSIOLOGY. 1995.

51. Penttonen M, Kamondi A, Sik A, Acsády L, Buzsáki G. Feed-forward and feed-back activation of the dentate gyrus in vivo during dentate spikes and sharp wave bursts. Hippocampus. 1997;7(4):437–50.

52. Lensu S, Waselius T, Penttonen M, Nokia MS. Dentate spikes and learning: disrupting hippocampal function during memory consolidation can improve pattern separation. J Neurophysiol. 2019;121:131–9.

53. Farrell JS, Soltesz I. Noncanonical circuits, states, and computations of the hippocampus. Science. 2025 Sept 11;389(6765):eadv4420.

54. Nokia MS, Gureviciene I, Waselius T, Tanila H, Penttonen M. Hippocampal electrical stimulation disrupts associative learning when targeted at dentate spikes. Journal of Physiology. 2017 July 15;595(14):4961–71.

55. Farrell JS, Hwaun E, Dudok B, Soltesz I. Neural and behavioural state switching during hippocampal dentate spikes. Nature. 2024 Apr 18;628(8008):590–5.

56. Bott JB, Muller MA, Jackson J, Aubert J, Cassel JC, Mathis C, et al. Spatial reference memory is associated with modulation of theta-gamma coupling in the dentate Gyrus. Cerebral Cortex. 2016 Sept 1;26(9):3744–53.

57. Dovek L, Ahmadi M, Marrero K, Zagha E, Santhakumar V. Cellular and circuit features distinguish dentate gyrus semilunar granule cells and granule cells activated during contextual memory formation. 2025 July 17 [cited 2026 Jan 1]; Available from: https://elifesciences.org/reviewed-preprints/101428v2

860 58. Maroso M, Balosso S, Ravizza T, Liu J, Aronica E, Iyer AM, et al. Toll-like receptor 4 and
861 high-mobility group box-1 are involved in ictogenesis and can be targeted to reduce
862 seizures. Nature Medicine. 2010 Apr;16(4):413–9.

863 59. Kleen JK, Holmes GL. Taming TLR4 may ease seizures. Nature Medicine. 2010
864 Apr;16(4):369–70.

865 60. Vezzani A, Balosso S, Ravizza T. Neuroinflammatory pathways as treatment targets and
866 biomarkers in epilepsy. Nat Rev Neurol. 2019 Aug;15(8):459–72.

867 61. Okun E, Griffioen KJ, Mattson MP. Toll-like receptor signaling in neural plasticity and
868 disease. Trends in Neurosciences. 2011 May;34(5):269–81.

869 62. Ahmad A, Crupi R, Campolo M, Genovese T, Esposito E, Cuzzocrea S. Absence of TLR4
870 Reduces Neurovascular Unit and Secondary Inflammatory Process after Traumatic
871 Brain Injury in Mice. Dhandapani KM, editor. PLoS ONE. 2013 Mar 28;8(3):e57208.

872 63. Xiong G, Metheny H, Johnson BN, Cohen AS. A comparison of different slicing planes in
873 preservation of major hippocampal pathway fibers in the mouse. Frontiers in
874 Neuroanatomy. 2017 Nov 21;11.

875 64. Howard AL, Neu A, Morgan RJ, Echegoyen JC, Soltesz I. Opposing Modifications in
876 Intrinsic Currents and Synaptic Inputs in Post-Traumatic Mossy Cells: Evidence for
877 Single-Cell Homeostasis in a Hyperexcitable Network. Journal of Neurophysiology.
878 2007 Mar;97(3):2394–409.

879 65. Dziembowska M, Milek J, Janusz A, Rejmak E, Romanowska E, Gorkiewicz T, et al.
880 Activity-Dependent Local Translation of Matrix Metalloproteinase-9. J Neurosci. 2012
881 Oct 17;32(42):14538–47.

882 66. Dziembowska M, Wlodarczyk J. MMP9: A novel function in synaptic plasticity. The
883 International Journal of Biochemistry & Cell Biology. 2012 May;44(5):709–13.

884 67. Stefaniuk M, Beroun A, Lebitko T, Markina O, Leski S, Meyza K, et al. Matrix
885 Metalloproteinase-9 and Synaptic Plasticity in the Central Amygdala in Control of
886 Alcohol-Seeking Behavior. Biological Psychiatry. 2017 June;81(11):907–17.

887 68. Szepesi Z, Hosy E, Ruszczycki B, Bijata M, Pyskaty M, Bikbaev A, et al. Synaptically
888 released matrix metalloproteinase activity in control of structural plasticity and the
889 cell surface distribution of GluA1-AMPA receptors. PLoS ONE. 2014 May 22;9(5).

890 69. Fanselow EE, Kubota Y, Wehr M, Yavorska I. Somatostatin-Expressing Inhibitory
891 Interneurons in Cortical Circuits. Frontiers in Neural Circuits | www.frontiersin.org.
892 2016;10:76.

70. Pirbhoy PS, Rais M, Lovelace JW, Woodard W, Razak KA, Binder DK, et al. Acute pharmacological inhibition of matrix metalloproteinase-9 activity during development restores perineuronal net formation and normalizes auditory processing in Fmr1 KO mice. Journal of Neurochemistry. 2020 Dec;155(5):538–58.

71. Sun DA, Deshpande LS, Sombati S, Baranova A, Wilson MS, Hamm RJ, et al. Traumatic brain injury causes a long-lasting calcium (Ca2+)-plateau of elevated intracellular Ca levels and altered Ca2+homeostatic mechanisms in hippocampal neurons surviving brain injury. Eur J of Neuroscience. 2008 Apr;27(7):1659–72.

72. Weber JT. Altered Calcium Signaling Following Traumatic Brain Injury. Front Pharmacol [Internet]. 2012 [cited 2025 Dec 22];3. Available from: http://journal.frontiersin.org/article/10.3389/fphar.2012.00060/abstract

73. Hellstrom IC, Danik M, Luheshi GN, Williams S. Chronic LPS exposure produces changes in intrinsic membrane properties and a sustained IL-β-dependent increase in GABAergic inhibition in hippocampal CA1 pyramidal neurons. Hippocampus. 2005;15(5):656–64.

74. Hainmueller T, Bartos M. Dentate gyrus circuits for encoding, retrieval and discrimination of episodic memories. Nature Reviews Neuroscience. 2020 Mar 1;21(3):153–68.

75. Hsu D. The dentate gyrus as a filter or gate: a look back and a look ahead. Prog Brain Res. 2007;163:601–13.

76. Ewell LA. To sleep perchance to spike: a functional role for dentate spikes in memory. Journal of Physiology. 2017 July 15;595(14):4565.

77. Farrell JS, Hwaun E, Dudok B, Soltesz I. Neural and behavioural state switching during hippocampal dentate spikes. [cited 2024 Mar 20]; Available from: https://doi.org/10.1038/s41586-024-07192-8

78. Flynn SP, Barrier S, Scott RC, Lenck-Santini PP, Holmes GL. Status epilepticus induced spontaneous dentate gyrus spikes: In vivo current source density analysis. PLoS ONE. 2015 July 6;10(7).

79. Engel J, Bragin A, Staba R. Nonictal EEG biomarkers for diagnosis and treatment. Epilepsia Open. 2018 Dec 1;3(S2):120–6.

80. Perucca P, Smith G, Santana-Gomez C, Bragin A, Staba R. Electrophysiological biomarkers of epileptogenicity after traumatic brain injury. Neurobiology of Disease. 2019 Mar;123:69–74.

81. Tewari BP, Chaunsali L, Campbell SL, Patel DC, Goode AE, Sontheimer H. Perineuronal nets decrease membrane capacitance of peritumoral fast spiking interneurons in a model of epilepsy. Nature Communications. 2018 Dec 1;9(1).

82. Whitebirch AC, LaFrancois JJ, Jain S, Leary P, Santoro B, Siegelbaum SA, et al. Enhanced excitability of the hippocampal CA2 region and its contribution to seizure activity in a mouse model of temporal lobe epilepsy. Neuron. 2022 Oct;110(19):3121-3138.e8.

934 **Figure legends:**

935 ***Figure 1: TLR4 signaling drives early excitatory and inhibitory synaptic changes in***
936 ***DGCs after brain injury.*** A) Schematic of the experimental question. B) Experimental
937 timeline for examining synaptic changes after FPI in rats. C) Representative sEPSC traces
938 showing whole-cell voltage clamp recordings from granule cells in vehicle treated sham
939 controls (black), vehicle treated FPI (red), TLR4 inhibited sham (grey) and TLR4 inhibited FPI
940 (blue). D-E) Cumulative probability plots comparing sEPSC interevent intervals (D) and
941 amplitude (E) between vehicle treated and TLR4 inhibited sham and injured rats. F)
942 Representative sIPSC traces showing whole-cell voltage clamp recordings from granule
943 cells in vehicle treated sham controls (black), vehicle treated FPI (red), TLR4 inhibited
944 sham (grey) and TLR4 inhibited FPI (blue). G-H) Cumulative probability plots comparing
945 sIPSC interevent intervals and amplitude between vehicle treated and TLR4 inhibited sham
946 and injured rats. I) Experimental timeline for examining synaptic changes after FPI in
947 $TLR4^{fl/fl}$: CaMKIIa- CreERT2 mice. J) Representative sEPSC traces from granule cells in Cre^{-ve}
948 sham controls (black), Cre^{-ve} FPI (red), Cre^{+ve} sham (grey) and Cre^{+ve} FPI (blue). K-L)
949 Cumulative probability plots comparing sEPSC interevent intervals and amplitude between
950 granule cells in Cre^{-ve} and Cre^{+ve} mice. * indicates $P<0.0001$ by K-S test.

951 ***Figure 2: TLR4 signaling upregulates MMP-9 activity in the dentate gyrus after brain***
952 ***injury.*** A) Experimental timeline for in-situ zymography to quantify MMP-9 activity after
953 brain injury in rat. B) Representative images showing MMP-9 activity in hippocampal
954 sections from sham and injured rats. Images from vehicle treated (middle) and TLR
955 inhibited mice (bottom) show MMP-9 activity in green. C) Quantification of MMP-9 activity,

956 normalized to CA1 stratum Radiatum, shows an increase in MMP-9 activity in vehicle
957 treated injured rats, but not in TAK-242 treated injured rats. Note that MMP-9 activity in
958 vehicle treated and TAK-242 treated sham rats were not different. D) Experimental timeline
959 for in-situ zymography to quantify MMP-9 activity after brain injury in mice. E)
960 Representative images showing MMP-9 activity in sham and injured mice. Images from
961 hippocampal sections from Cre^{-ve} sham and injured mice (top) and Cre^{+ve} sham and injured
962 mice (bottom) show MMP-9 activity in green.F) Quantification of MMP-9 activity, normalized
963 to CA1 stratum Radiatum, shows an increase in MMP-9 activity after brain injury in Cre^{-ve}
964 mice, but not in Cre^{+ve} mice. Note that MMP-9 activity in sham mice was not different. *
965 indicates $P<0.05$ by TW-ANOVA with Šídáks multiple comparisons post hoc tests. G)
966 Experimental timeline for RNAscope experiments in naïve rats. H) Representative images
967 showing increase in MMP-9 mRNA in sections from rats after LPS-B5 treatment. I)
968 Summary plot of mRNA levels in saline, LPS-B5 treated and LPS-B5+JSH-23 sections
969 shows an increase in mRNA levels after LPS-B5 treatment which is abolished by blocking
970 NF-κB. * indicates $P<0.05$ by OW-ANOVA with Šídáks multiple comparisons post hoc tests.

971 ***Figure 3: Blocking MMP-9 prevents early synaptic changes in excitatory inputs to DGCs***
972 ***after brain injury.*** A) Experimental timeline for examining synaptic changes in acute rat
973 slices after LPS incubation. B) Representative sEPSC traces from granule celsl in LPS
974 incubated (orange), LPS+SB-3CT co-incubated (magenta) slices. C-D) Cumulative
975 probability plots comparing sEPSC interevent intervals and amplitude between LPS-B5
976 incubated and LPS-B5+SB-3CT co-incubated slices. Note that LPS incubation significantly
977 reduced interevent intervals. Co-incubation of slices in MMP-9 blocker SB-3CT prevented

978 this change and were not different from sham animals. MMP-9 inhibition did not rescue
979 changes in sEPSC amplitude. E) Experimental timeline for examining synaptic changes in
980 SB-3CT treated sham/injured rats. F) Representative granule cell sEPSC traces showing
981 from SB-3CT treated sham (grey) and injured rats (green). G-H) Cumulative probability plots
982 comparing sEPSC interevent intervals and amplitude between SB-3CT treated
983 sham/injured rats. I) Experimental timeline for examining synaptic changes in SB-3CT
984 treated mice after brain injury. J) Representative granule cell sEPSC traces from vehicle
985 treated (red) and SB-3CT treated mice(green). K-L) Cumulative probability plots comparing
986 sEPSC interevent intervals and amplitude between vehicle treated and SB-3CT treated
987 mice. * indicates $P<0.0001$ by K-S test.

988 ***Figure 4: TLR4 regulation of MMP-9 activity enhances dentate network excitability after***
989 ***brain injury.*** A) Experimental timeline for *in vivo* experiments examining dentate excitability
990 and throughput. B) Representative traces showing DG population spike from sham and
991 injured animals in response to 800 μA stimulus (bold lines) and 1200 μA (dotted lines). C)
992 Input-output curve illustrating early saturation of population spike amplitude in injured
993 animals (red) compared to sham controls. D) Inhibition of TLR4 or MMP-9 effectively
994 mitigates these changes. E) MMP-9 inhibition (light grey) did not affect input-output curves
995 in sham animals, TLR4 inhibition increased network excitability of sham animals (grey). F)
996 Representative trace from 16 channel silicon probe recording local field potentials from
997 cortex to hippocampus. Current-source density plot shows the sink and source of an
998 individual dentate spike. inset- a single dentate spike recorded in the GC layer. G)
999 Quantification of dentate spikes shows a significant increase in frequency in injured

1000 animals. Note that inhibition of TLR4 or MMP-9 effectively reduced changes in dentate
1001 spike frequency in injured animals. * indicates<0.05 by TW-ANOVA with Šídáks multiple
1002 comparisons post hoc tests.

1003 ***Figure 5: Posttraumatic deficits in long-term potentiation is improved by early***
1004 ***inhibition of TLR4 or MMP-9.*** A) Experimental timeline for *in vivo* assessment of long-term
1005 potentiation in perforant path synapses to DGCS. B-C) Injured rats exhibit a significant
1006 decrease in fEPSP slope values after 60 minutes(red) compared to sham controls (black).
1007 D-E) Inhibition of TLR4 (blue) or MMP-9 (green) significantly improved LTP in injured
1008 animals. F-G) MMP-9 inhibition did not affect LTP in SHAM controls. TLR4 inhibition
1009 reduced LTP at 60 min and 180 min after induction. * indicates *P* <0.05 by TW-RM ANOVA.

1010 ***Figure 6: Early inhibition of TLR4 or MMP-9 improves spatial learning after brain injury.***
1011 A) Experimental timeline for testing spatial learning using Barnes maze. B) Representative
1012 heat plot showing rats trajectory during the task on day 2. C-E) Injured animals showed
1013 deficits in latency to escape, distance travelled, and search strategy on day 2. * indicates
1014 P<0.05 by RM-ANOVA. F-H) Summary plots of effect of TLR4 or MMP-9 inhibition on latency
1015 to escape (F), distance travelled (G), and search strategy (H) on day 2. I) Injured animals
1016 showed increased thigmotaxis on day 2 which was reduced with TLR4 or MMP-9 inhibition.
1017 * indicates P<0.05 by TW-ANOVA with Šídáks multiple comparisons post hoc tests.

1018

1019 ***Figure 7: Graphical Summary of TLR4 regulation of dentate gyrus function in control***

1020 ***and injured brain.***

1021 In uninjured brain, pharmacological inhibition of TLR4 signaling increases the frequency of

1022 both excitatory and inhibitory currents and enhances network excitability and impairs long-

1023 term potentiation without altering MMP-9 activity. Genetic deletion of neuronal TLR4 alters

1024 intrinsic properties without impacting synaptic physiology. Together these data are

1025 consistent with glial TLR4 signaling contributing to basal synaptic homeostasis in line with

1026 prior ex vivo studies [14].In the injured brain, augmented neuronal TLR4 signaling acts

1027 through MMP-9 to enhance glutamatergic signaling, network excitability and dentate spikes

1028 and impairs LTP maintenance. Mechanistically, inhibitory changes are driven by TLR4 in an

1029 MMP-9 independent manner. Together, these findings demonstrate that TLR4 signaling

1030 regulates DG function and seizure susceptibility [13] through distinct, context-dependent

1031 cellular mechanisms in the healthy and injured brain.

1032

1033

FIGURE.1

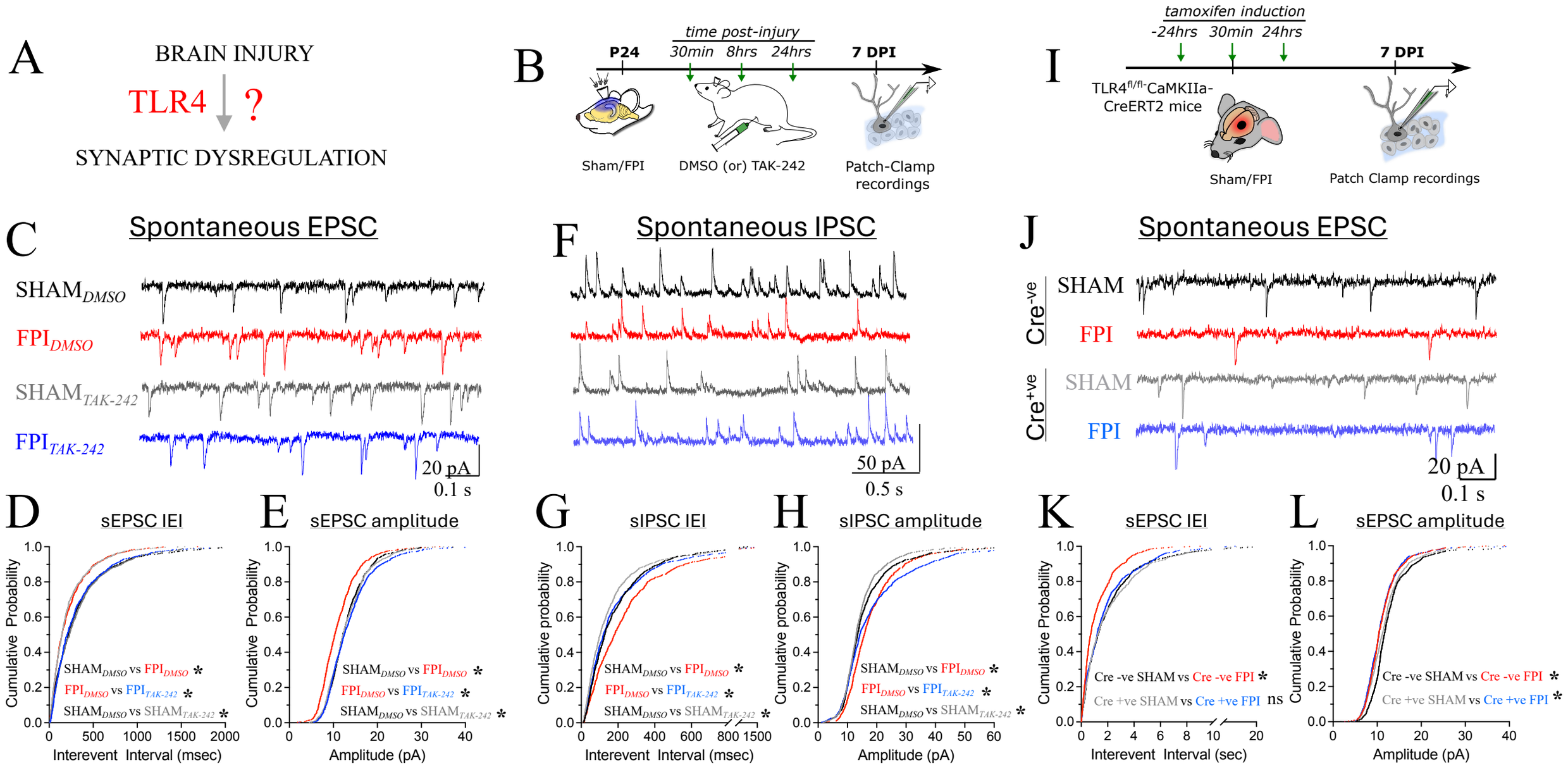
A
BRAIN INJURY
TLR4 ?
SYNAPTIC DYSREGULATION
B
time post-injury
P24
30min 8hrs 24hrs
7 DPI
Sham/FPI
DMSO (or) TAK-242
Patch-Clamp recordings
I
tamoxifen induction
-24hrs 30min 24hrs
7 DPI
TLR4fl/fl-CaMKIIa-CreERT2 mice
Sham/FPI
Patch Clamp recordings
C
Spontaneous EPSC
SHAMDMSO
FPIDMSO
SHAMTAK-242
FPITAK-242
20 pA
0.1 s
F
Spontaneous IPSC
50 pA
0.5 s
J
Spontaneous EPSC
Cre-ve
SHAM
FPI
Cre+ve
SHAM
FPI
20 pA
0.1 s
D
sEPSC IEI
Cumulative Probability
SHAMDMSO vs FPIDMSO *
FPIDMSO vs FPITAK-242 *
SHAMDMSO vs SHAMTAK-242 *
Interevent Interval (msec)
E
sEPSC amplitude
Amplitude (pA)
G
sIPSC IEI
Cumulative probability
Interevent Interval (msec)
H
sIPSC amplitude
Amplitude (pA)
K
sEPSC IEI
Cre -ve SHAM vs Cre -ve FPI *
Cre +ve SHAM vs Cre +ve FPI ns
Interevent Interval (sec)
L
sEPSC amplitude
Cre -ve SHAM vs Cre -ve FPI *
Cre +ve SHAM vs Cre +ve FPI *
Amplitude (pA)

FIGURE.2

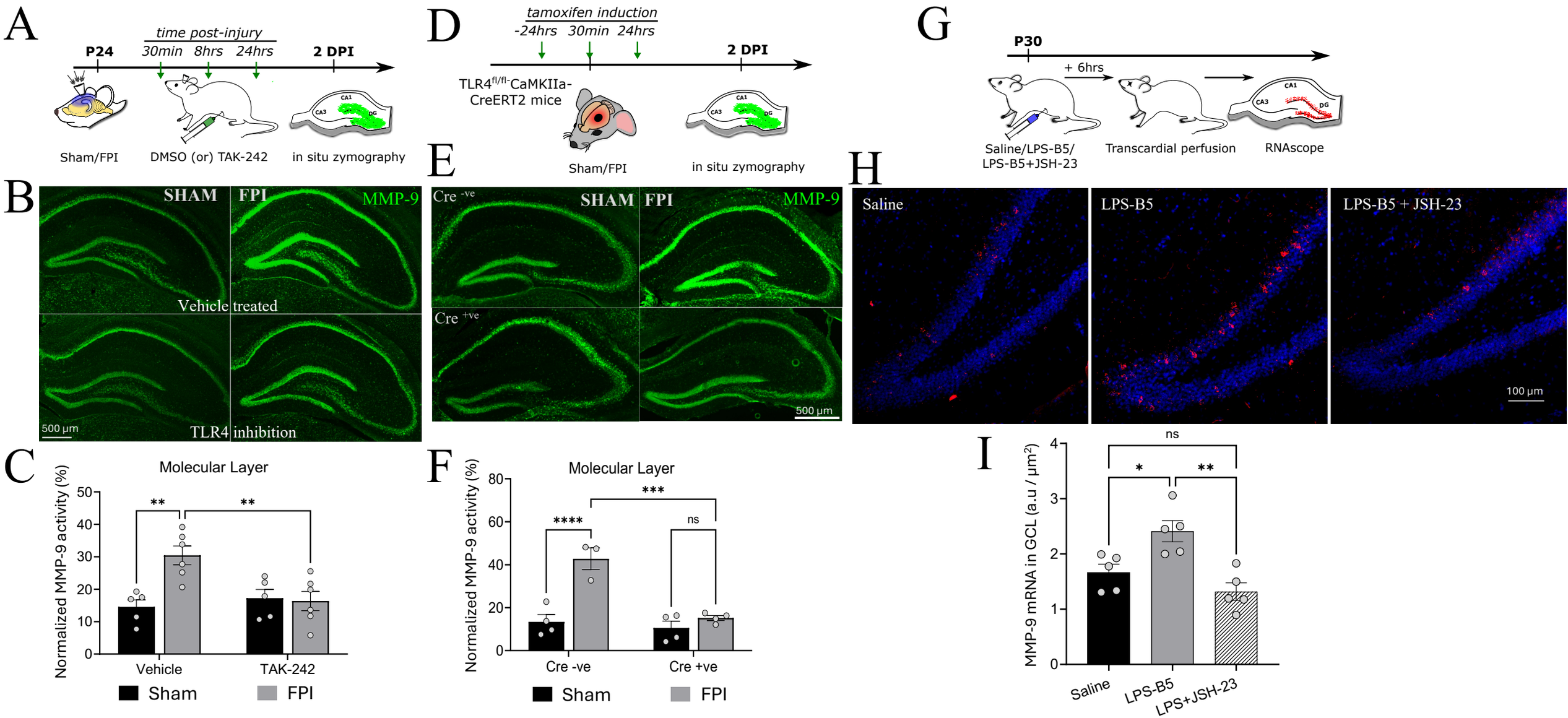
A
time post-injury
P24
30min
8hrs
24hrs
2 DPI
Sham/FPI
DMSO (or) TAK-242
in situ zymography
B
SHAM
FPI
MMP-9
Vehicle treated
TLR4 inhibition
500 µm
C
Molecular Layer
Normalized MMP-9 activity (%)
Vehicle
TAK-242
Sham
FPI
D
tamoxifen induction
-24hrs
30min
24hrs
2 DPI
TLR4fl/fl-CaMKIIa-CreERT2 mice
Sham/FPI
in situ zymography
E
Cre -ve
Cre +ve
SHAM
FPI
MMP-9
500 µm
F
Molecular Layer
Normalized MMP-9 activity (%)
Cre -ve
Cre +ve
Sham
FPI
G
P30
+ 6hrs
Saline/LPS-B5/
LPS-B5+JSH-23
Transcardial perfusion
RNAscope
H
Saline
LPS-B5
LPS-B5 + JSH-23
100 µm
I
MMP-9 mRNA in GCL (a.u / µm²)
ns
Saline
LPS-B5
LPS+JSH-23

FIGURE.3

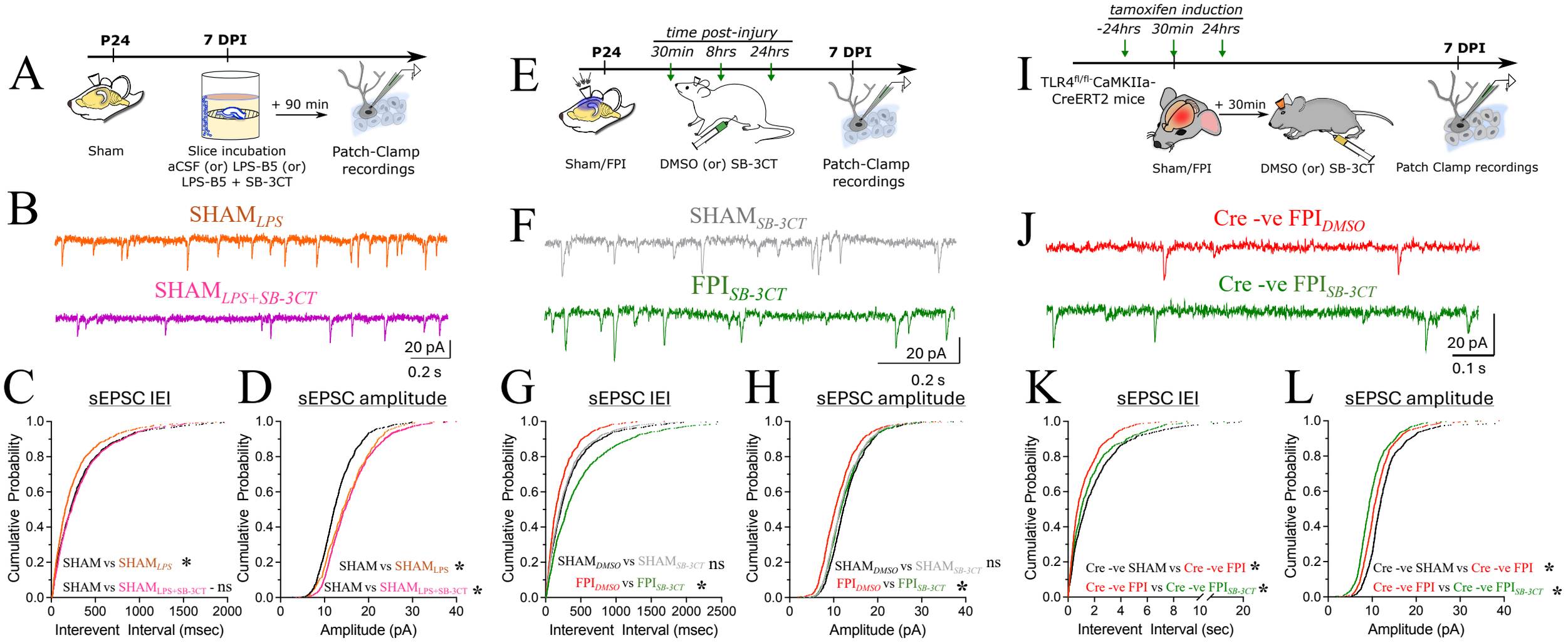
A
P24
7 DPI
+ 90 min
Sham
Slice incubation
aCSF (or) LPS-B5 (or)
LPS-B5 + SB-3CT
Patch-Clamp
recordings
B
SHAM$_{LPS}$
SHAM$_{LPS+SB-3CT}$
20 pA
0.2 s
C
sEPSC IEI
Cumulative Probability
SHAM vs SHAM$_{LPS}$ *
SHAM vs SHAM$_{LPS+SB-3CT}$ - ns
Interevent Interval (msec)
D
sEPSC amplitude
SHAM vs SHAM$_{LPS}$ *
SHAM vs SHAM$_{LPS+SB-3CT}$ *
Amplitude (pA)
E
time post-injury
P24
30min 8hrs 24hrs
7 DPI
Sham/FPI
DMSO (or) SB-3CT
Patch-Clamp
recordings
F
SHAM$_{SB-3CT}$
FPI$_{SB-3CT}$
20 pA
0.2 s
G
sEPSC IEI
SHAM$_{DMSO}$ vs SHAM$_{SB-3CT}$ ns
FPI$_{DMSO}$ vs FPI$_{SB-3CT}$ *
Interevent Interval (msec)
H
sEPSC amplitude
SHAM$_{DMSO}$ vs SHAM$_{SB-3CT}$ ns
FPI$_{DMSO}$ vs FPI$_{SB-3CT}$ *
Amplitude (pA)
I
tamoxifen induction
-24hrs 30min 24hrs
7 DPI
TLR4$^{fl/fl}$-CaMKIIa-
CreERT2 mice
+ 30min
Sham/FPI
DMSO (or) SB-3CT
Patch Clamp recordings
J
Cre -ve FPI$_{DMSO}$
Cre -ve FPI$_{SB-3CT}$
20 pA
0.1 s
K
sEPSC IEI
Cre -ve SHAM vs Cre -ve FPI *
Cre -ve FPI vs Cre -ve FPI$_{SB-3CT}$ *
Interevent Interval (sec)
L
sEPSC amplitude
Cre -ve SHAM vs Cre -ve FPI *
Cre -ve FPI vs Cre -ve FPI$_{SB-3CT}$ *
Amplitude (pA)

FIGURE.4

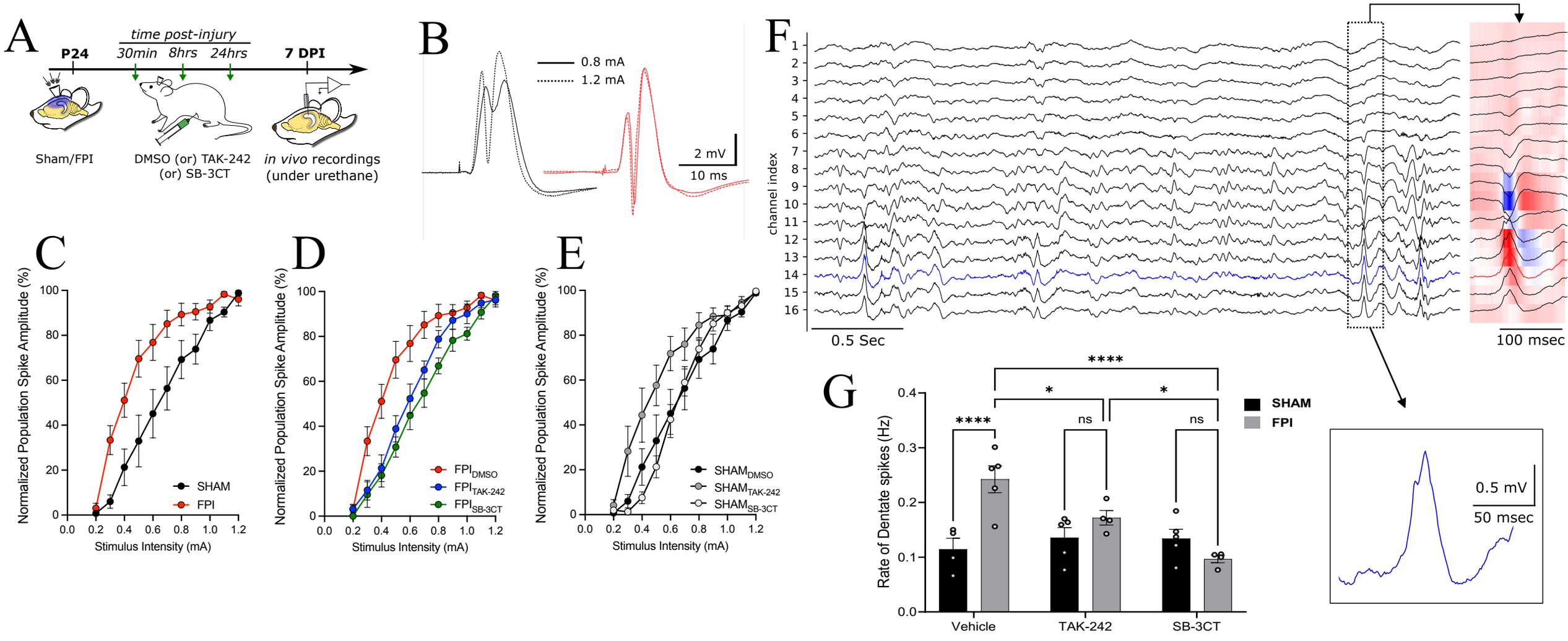
A
time post-injury
P24
30min
8hrs
24hrs
7 DPI
Sham/FPI
DMSO (or) TAK-242 (or) SB-3CT
in vivo recordings (under urethane)
B
0.8 mA
1.2 mA
2 mV
10 ms
C
D
E
Normalized Population Spike Amplitude (%)
Stimulus Intensity (mA)
SHAM
FPI
FPI DMSO
FPI TAK-242
FPI SB-3CT
SHAM DMSO
SHAM TAK-242
SHAM SB-3CT
F
channel index
0.5 Sec
100 msec
G
Rate of Dentate spikes (Hz)
Vehicle
TAK-242
SB-3CT
SHAM
FPI
****
*
ns
0.5 mV
50 msec

FIGURE.5

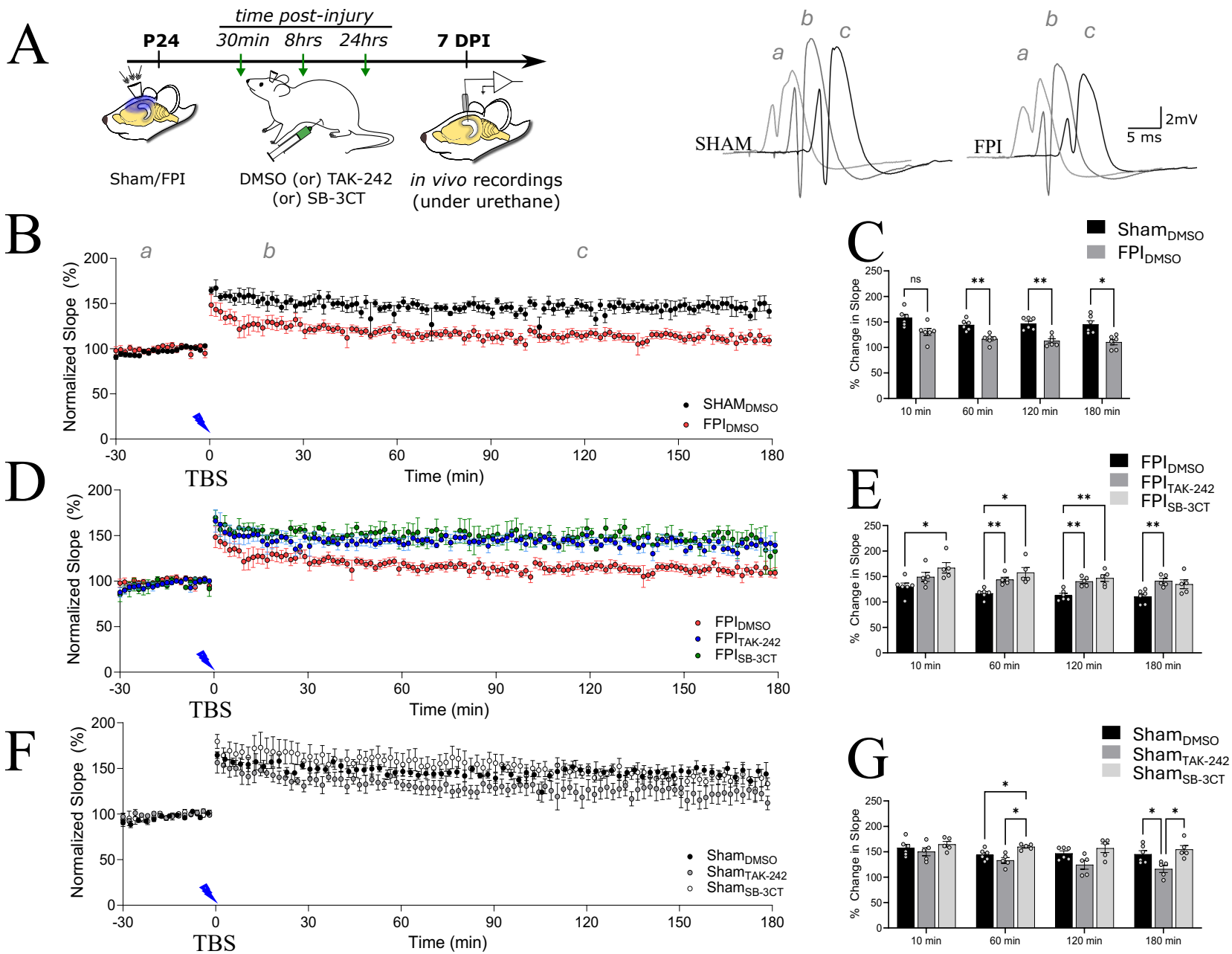
A
time post-injury
P24
30min
8hrs
24hrs
7 DPI
Sham/FPI
DMSO (or) TAK-242
(or) SB-3CT
in vivo recordings
(under urethane)
a
b
c
SHAM
FPI
2mV
5 ms
B
Normalized Slope (%)
Time (min)
TBS
SHAM_DMSO
FPI_DMSO
C
Sham_DMSO
FPI_DMSO
% Change in Slope
ns
10 min
60 min
120 min
180 min
D
FPI_DMSO
FPI_TAK-242
FPI_SB-3CT
E
F
Sham_DMSO
Sham_TAK-242
Sham_SB-3CT
G

FIGURE.6

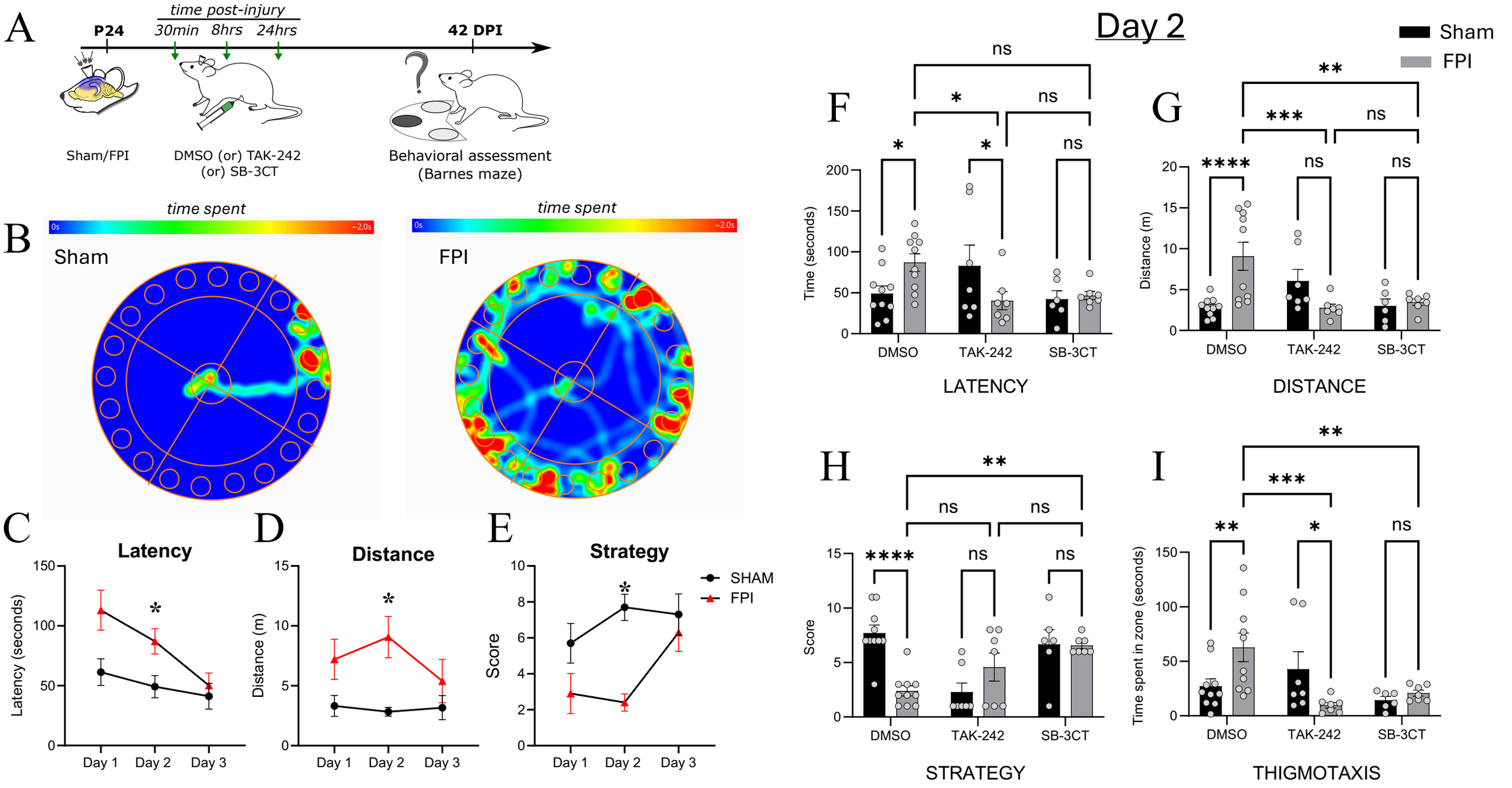
A
time post-injury
P24
30min
8hrs
24hrs
42 DPI
Sham/FPI
DMSO (or) TAK-242
(or) SB-3CT
Behavioral assessment
(Barnes maze)
B
time spent
0s
~2.0s
Sham
FPI
C
Latency
Latency (seconds)
Day 1
Day 2
Day 3
D
Distance
Distance (m)
E
Strategy
Score
SHAM
FPI
Day 2
Sham
FPI
F
Time (seconds)
DMSO
TAK-242
SB-3CT
LATENCY
G
Distance (m)
DISTANCE
H
Score
STRATEGY
I
Time spent in zone (seconds)
THIGMOTAXIS
ns

FIGURE.7

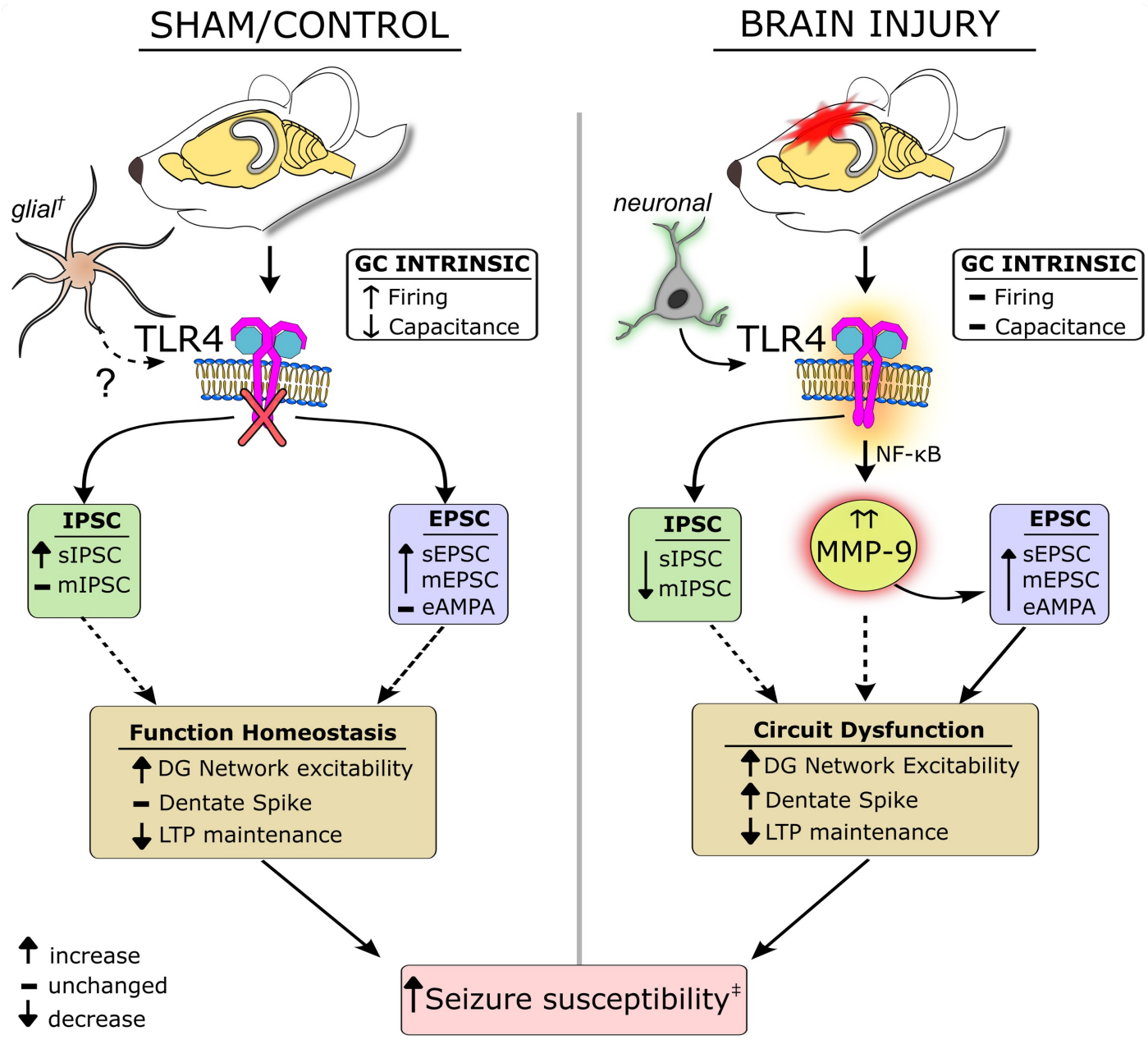
SHAM/CONTROL
BRAIN INJURY
glial†
?
TLR4
GC INTRINSIC
↑ Firing
↓ Capacitance
IPSC
↑ sIPSC
– mIPSC
EPSC
↑ sEPSC
mEPSC
– eAMPA
Function Homeostasis
↑ DG Network excitability
– Dentate Spike
↓ LTP maintenance
neuronal
TLR4
GC INTRINSIC
– Firing
– Capacitance
NF-κB
IPSC
↓ sIPSC
mIPSC
↑↑
MMP-9
EPSC
↑ sEPSC
mEPSC
eAMPA
Circuit Dysfunction
↑ DG Network Excitability
↑ Dentate Spike
↓ LTP maintenance
↑ increase
– unchanged
↓ decrease
↑Seizure susceptibility‡